

The Pionic Fabric and Quark Molecular Dynamics

Rami Rom^(a)

Abstract: Similar to Harari's Rishon particles model that described all leptonic and baryonic matter composed of four substructure fundamental particles and antiparticles, $T, V, \tilde{T}, \tilde{V}$, we propose that the four quarks and antiquarks, $u, d, \tilde{u}, \tilde{d}$ are the substructure building blocks of all particles and also the substructure of the vacuum pionic fabric. We develop a classical and quantum hybrid quark molecular dynamics scheme to study the pionic fabric. In free space, the pionic fabric zero-energy unit cell is cubic and includes two flipped pion tetrahedrons. Protons and neutrons contract and curve the pionic fabric cells and we calculate the pionic fabric density as a function of distance from an embedded proton in a pionic fabric cell. Based on the β decay, we propose that electrons are non-elementary, non-point like particles having a similar substructure to the pionic fabric cell and form together electron clouds. Motion of the electron in the pionic fabric is performed by a u and d quark exchanges via tunneling through a double well potential barrier in the ground state. The rapid quark exchanges transform the electron tetraquarks into pion tetraquarks and vice versa. After the u and d quark exchanges, the zero-energy pionic unit cell contracts by a factor of 5 and the embedded electron pionic cell energy is equal to the electron rest mass of 0.511 MeV. Finally, we propose a new interpretation to QED based on the pionic fabric structure and dynamics. Lattice QCD computations may allow calculating the mass of the pionic fabric unit cell and the embedded electron pionic cell.

Keywords: Antimatter, Quantum vacuum, Lattice QCD and Exotic Tetraquark

(a) Email: romrami@gmail.com

1. Introduction - Some Quantum Theory Difficulties

- (a) According to the standard model of particle physics the building blocks of the universe are quantum fields. Quantum fields have no bodies and no limits, exist everywhere in space all the time and hence may overlap and do not occupy or exclude other quantum fields. The quantum fields are abstract and virtual mathematical objects and are inconsistent with atomistic point of view where the fundamental building blocks of the universe are physical particles.
- (b) Schrödinger's electron wavepacket width grows linearly with time in free space - Erwin Schrödinger introduced the idea of a particle wave packet and the superposition of eigenfunctions and found that a gaussian wavepacket remains compact for a quantum harmonic oscillator¹. However, Schrödinger found that in free space the width of the gaussian wavepacket grows linearly with time. If an electron wavepacket is initially localized in a region of an atomic dimension of 10^{-10} meters, the width of the wavepacket doubles in about 10^{-16} seconds and after about a milli-second the wave packet width grows to about a kilometer².
- (c) Dirac's negative energy states make the electron positive energy states unstable – Paul Dirac proposed a relativistic wave equation and found a new set of negative energy antimatter states³. Dirac thought that since the positive energy electron solutions would decay to the negative energy states there must be an infinite number of invisible electrons that occupy the negative states and prevent the electron decay based on Pauli exclusion principle⁴.
- (d) The standard model of particle physics assumes that the electron is an elementary point-like particle with infinite mass and charge densities, however, Dirac assumed that electrons are not point like particles and proposed a spherical shell electron model⁵.

- (e) Feynman's integrals for the electron self-energy and the vacuum polarization diverge - Robert Oppenheimer showed that the vacuum polarization and the electron self-energy are not small perturbative corrections. Paul Dirac and Richard Feynman did not like the renormalization scheme that succeeded to cancel these infinities. Dirac thought that electrons interact strongly with the vacuum electron-positron virtual pairs and hence are never bare in contrast to Feynman's diagrams, where bare electrons propagate in free space in zero-order⁶⁻⁷. Dirac thought that better understanding of the vacuum structure is needed for the quantum electron theory⁸.
- (f) Harari suggested a model where leptonic and baryonic particles (protons, neutrons, electrons and also the interaction bosons, $w^{+/-}$ and Z) are composite particles. Harari named the proposed substructure fundamental particles Rishons, T and V , having an electric charge of a $1/3$ and a 0 . Various combinations of rishons and their anti-rishons create the leptons and hadrons. According to Harari, all particles consist of the two fundamental particles and their anti-particles $T, V, \tilde{T}, \tilde{V}$ ⁹.

At least these quantum theory difficulties indicate that new models beyond the standard model of particle physics could be considered.

2. The Addressed Questions

The questions we address in this paper are:

1. Does the quantum vacuum have substructure pionic unit cell?
2. Are the four quarks and antiquarks $u, d, \tilde{d}, \tilde{u}$, the fundamental substructure building blocks of leptons and hadrons?
3. Do the non-elementary, non-point like electrons move in the pionic fabric by rapid u and d quark exchanges?

3. The Pion Tetrahedron and the Vacuum Substructure

We assume that the quantum vacuum is filled with exotic pion tetraquark tetrahedron particles that form a fabric¹⁰⁻¹⁴. We note that the vacuum pion tetraquark tetrahedrons are not ordinary particles since they are composed of 50% antiquarks and 50% quarks. We assume that the pion quarks and antiquarks do not annihilate each other, and that their dynamics may be modeled with classical molecular dynamics with additional quark exchange operation described below. We assume that the pionic fabric unit cell includes two exotic tetraquark particles, $u\tilde{d}d\tilde{u}$, each composed of the two light quarks, d and u , and their antiquark pairs, \tilde{d} and \tilde{u} . We first describe the classical and quantum hybrid quark molecular dynamics scheme for the pion tetraquark tetrahedrons and the pionic fabric unit cell and then describe electron-pion clouds, positron tetraquarks, electron-positron creation and decay to pions and a proton embedded in a pion cell.

The Classical and Quantum Hybrid Quark Molecular Dynamics Scheme

The pion tetraquark molecule is assumed to be composed of a $d\tilde{d}$ and $u\tilde{u}$ mesons having a tetrahedron structure shown in figure 2 where the cubic cell size a_π is a free parameter that will be determined by the classical and quantum hybrid quark molecular dynamics scheme described below. Two pion tetraquark tetrahedron enantiomers may exist obtained by exchanging the positions of two quarks at the tetrahedron vertices that breaks dynamically the chiral symmetry assumed by the effective field QCD theory¹⁵⁻²¹.

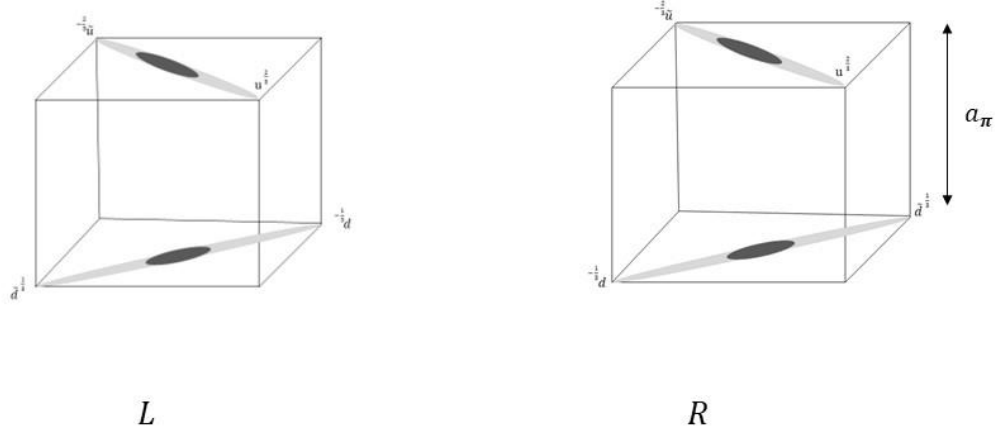


Figure 2 illustrates two pion tetraquark tetrahedron enantiomers.

The pion tetraquark Hamiltonian using quark pair interaction model²² is –

$$\begin{aligned}
 H_{\text{pion tetraquark}} = & \frac{1}{2} m_u v_u^2 + \frac{1}{2} m_{\bar{u}} v_{\bar{u}}^2 + \frac{1}{2} m_d v_d^2 + \frac{1}{2} m_{\bar{d}} v_{\bar{d}}^2 - \frac{4}{9} \frac{e^2}{4\pi \epsilon_0 r_{u,\bar{u}}} + \sigma_{u,u} r_{\bar{u},u} + \\
 & \frac{2}{9} \frac{e^2}{4\pi \epsilon_0 r_{u,\bar{d}}} + \sigma_{u,d} r(u, \bar{d}) - \frac{2}{9} \frac{e^2}{4\pi \epsilon_0 r_{u,d}} + \sigma_{u,d} r_{u,d} + \frac{2}{9} \frac{e^2}{4\pi \epsilon_0 r_{\bar{u},d}} + \sigma_{u,d} r_{\bar{u},d} - \frac{2}{9} \frac{e^2}{4\pi \epsilon_0 r_{\bar{u},\bar{d}}} + \\
 & \sigma_{u,d} r_{\bar{u},\bar{d}} - \frac{2}{9} \frac{e^2}{4\pi \epsilon_0 r_{d,\bar{d}}} + \sigma_{d,d} r_{d,\bar{d}} \quad (4)
 \end{aligned}$$

The hybrid classical and quantum quark molecular dynamics scheme includes in addition to solving Newtonian classical dynamics equations for the four quarks and antiquarks, quark exchange operations which are beyond classical mechanics. We assume that an Active Gluonic Center (AGC) is created in the center of hadrons by the quark and antiquark interaction where

quark and antiquark pairs are annihilated and then re-created, exchanging positions and flipping the velocities of the quark pair according to equations 6a-b below. The quark exchanges at the AGC prevents the quarks falling into the attractive coulomb singularity at very short distances $r_{q,\bar{q}} \sim 0$. The quarks and antiquarks continue their periodic trajectories following exactly the path of their pair quark after the exchange.

$$\vec{r}_q(t+1) = \vec{r}_{\bar{q}}(t), \quad \vec{r}_{\bar{q}}(t+1) = \vec{r}_q(t) \quad (6a)$$

$$\vec{v}_q(t+1) = -\vec{v}_{\bar{q}}(t), \quad \vec{v}_{\bar{q}}(t+1) = -\vec{v}_q(t) \quad (6b)$$

An example of the pion tetraquark trajectory is shown in figure 3. The two-meson quark and antiquark, $u\tilde{u}$ and $\tilde{d}d$, are attracted to each other and two quark exchange operations at the pion AGC are shown below where the trajectories of the \tilde{u} (in blue) and u (in orange) occurs simultaneously with the switching of the \tilde{d} (in green) and d quarks trajectories (in red). The annihilation and creation of the quark and antiquark at the AGC surface occurs instantly in a single propagation time step and the classical trajectory continues using Newtonian classical dynamics.

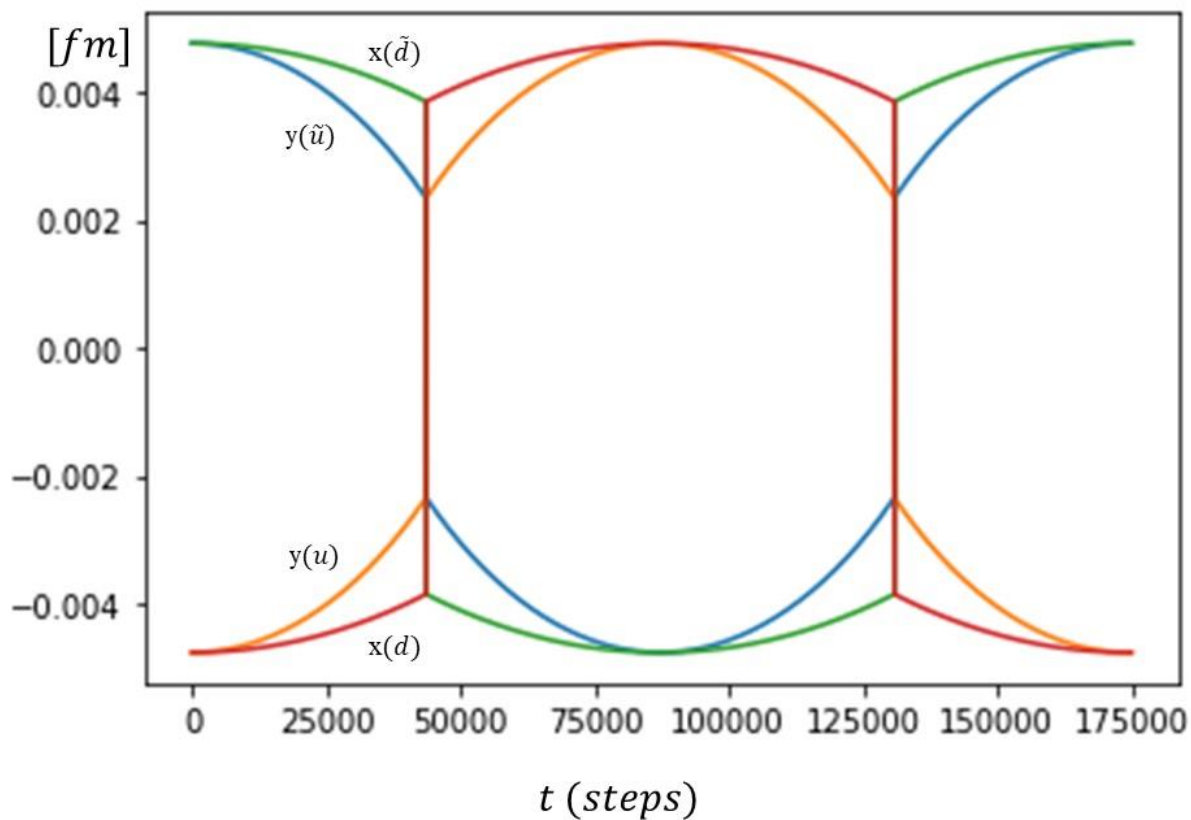


Figure 3 illustrates the exotic pion tetraquark tetrahedron trajectory with the quark exchanges at the pion gluonic center (AGC).

Since the pion quarks exchange positions periodically, the two pion tetrahedron enantiomers shown in figure 2 are mixed dynamically. The tetrahedron chiral symmetry is broken dynamically as expected from the ground state vacuum expectation value (VEV) by effective field QCD theory¹⁵⁻²².

4. The Pion Cell and the Vacuum Fabric Structure

A pionic cubic cell that fill space may be built from two rotated and flipped pion tetraquark tetrahedrons as shown below. The eight up, down, anti-up and anti-down quarks capture the 8 vertices of the pionic cell where on the six faces of the cube there is a chargeless and colorless pion, $\tilde{u} d \tilde{d} u$. We assign the indices below to the first pion (1,2,3,4) and the second inverted pion (5,6,7,8).

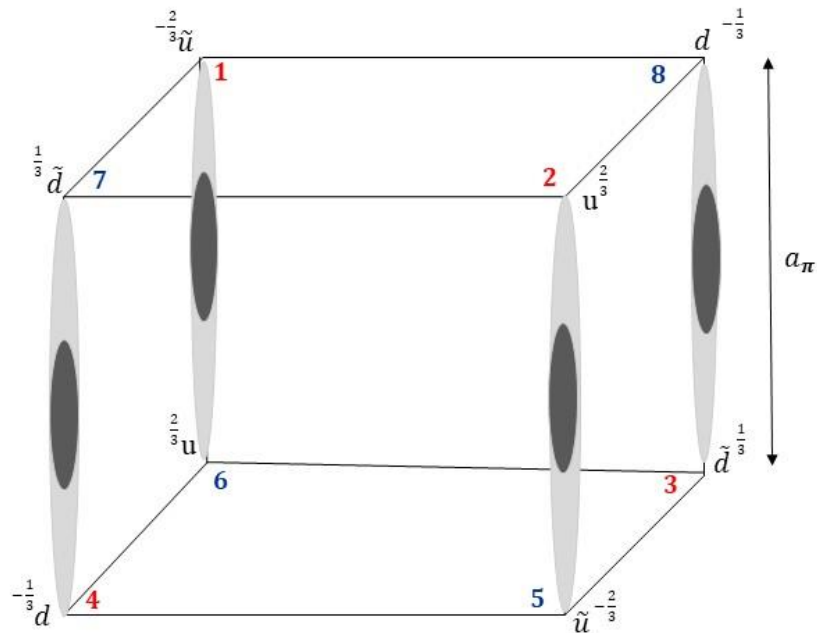


Figure 4 illustrates the pionic fabric cubic unit cell built from two flipped pion tetraquark tetrahedrons.

As can be seen in figure 5, d quark (5) has two \tilde{u} and two u quarks surrounding it in the X-Y plane and two \tilde{d} quarks in the Z direction. Similarly, u quark (2) is surrounded by two \tilde{d} and two d quarks in the X-Y plane and two \tilde{u} quarks in the Z direction. The \tilde{d} and \tilde{u} quarks (3 and 1) have similar quark pair structure in the pion unit cell and its nearest neighbors in the pionic fabric.

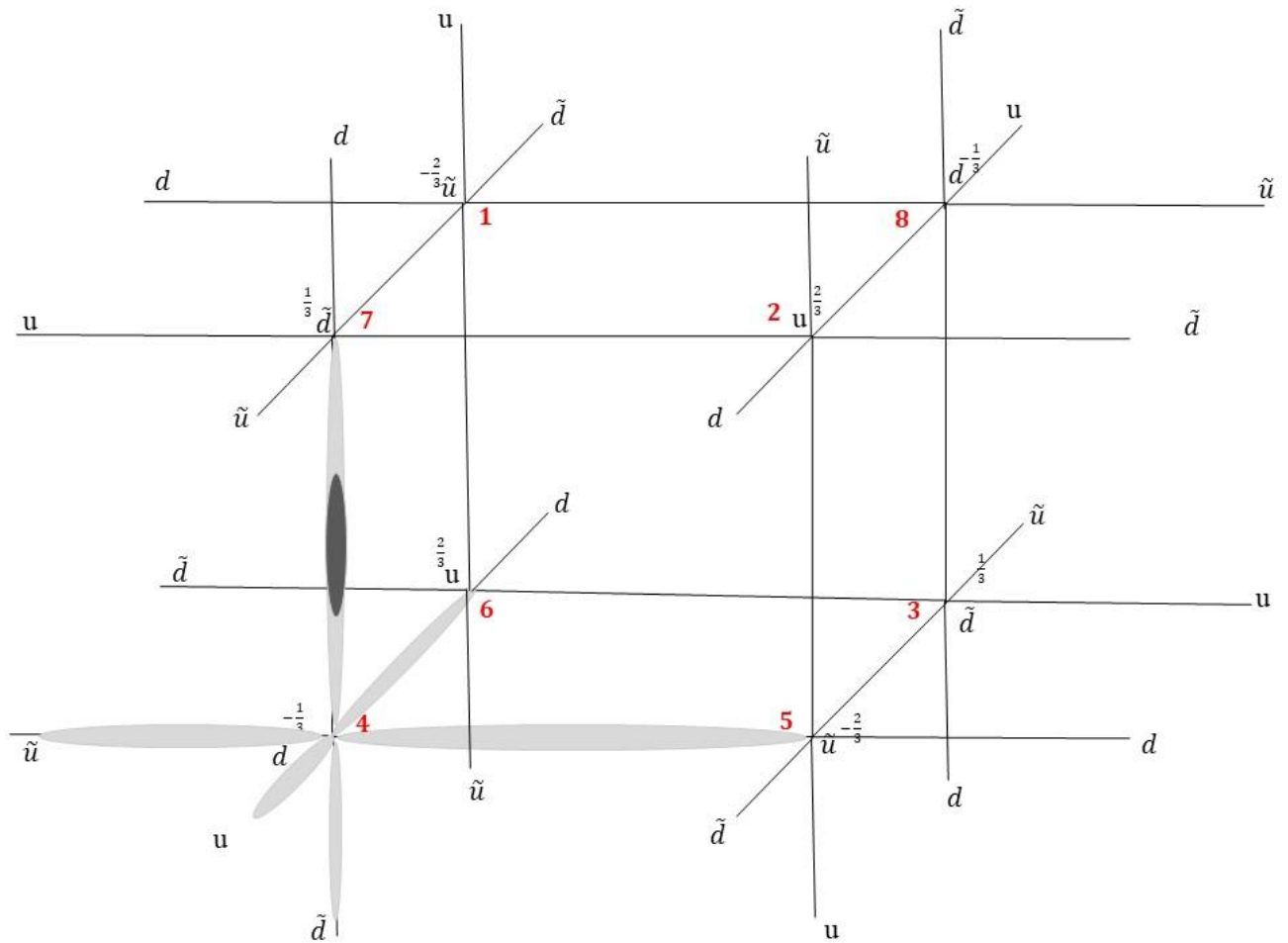


Figure 5 illustrates the pionic fabric cubic unit cell and nearest neighbors in the pionic fabric.

The Hamiltonian for the pion cell includes a sum of pair potentials²² between all 8 quarks and antiquarks where the sign and magnitude of the Coulomb interaction terms $q_{i,j}$ and the strength of the string tensions $\sigma_{i,j}$ are given below.

$$H_{pion\ cell} = \sum_{i=1}^8 \frac{1}{2} m_i v_i^2 + \sum_{i,j=1(i < j)}^8 \left(\frac{q_{i,j} e^2}{4\pi \epsilon_0 r_{i,j}} + \sigma_{i,j} r_{i,j} \right) \quad (7)$$

$$q_{i,j} = \begin{aligned} & -\frac{4}{9} \text{ for } \tilde{u} u \text{ pairs} \\ & \frac{4}{9} \text{ for } \tilde{u} \tilde{u} \text{ and } uu \text{ pairs} \\ & -\frac{2}{9} \text{ for } u d \text{ and } \tilde{u} \tilde{d} \text{ pairs} \\ & \frac{2}{9} \text{ for } \tilde{u} d \text{ and } \tilde{d} u \text{ pairs} \\ & -\frac{1}{9} \text{ for } d \tilde{d} \text{ pair} \\ & \frac{1}{9} \text{ for } d d \text{ and } \tilde{d} \tilde{d} \text{ pairs} \end{aligned} \quad (8)$$

$$\sigma_{i,j} = \begin{aligned} & \sigma_{u,u} \text{ for } \tilde{u} u, \tilde{u} \tilde{u} \text{ and } uu \text{ pairs} \\ & \frac{\sigma_{u,u}}{2} \text{ for } \tilde{u} d, \tilde{u} \tilde{d}, \tilde{u} d \text{ and } u\tilde{d} \text{ pairs} \\ & \frac{\sigma_{u,u}}{4} \text{ for } \tilde{d} d, \tilde{d} \tilde{d}, \text{ and } dd \text{ pairs} \end{aligned} \quad (9)$$

The total energy of the pionic fabric unit cell should vanish exactly and the following equation for the cube cell length $a_{pion\ cell}$ as a function of the string tension parameter $\sigma_{u,u}$ provides the zero-energy pion cell length that can fill space with infinite number of the zero-energy pion cells.

$$a_{pion\ cell} = \sqrt{\frac{\left(\frac{10}{9}\left(1-\left(\frac{1}{\sqrt{3}}-1\right)\sqrt{2}\right)\hbar c \alpha\right)}{2\left(\frac{26}{4}+\left(\frac{13}{2}+\frac{5}{2\sqrt{3}}\right)\frac{1}{\sqrt{2}}\right)\sigma_{u,u}}} \quad (10)$$

The value of the vacuum pionic cell AGC string tension parameter $\sigma_{u,u} = 1.5 \text{ KeV/fm}$ is determined such that the vibration frequency of the pionic unit cell quarks and antiquarks will be equal to Dirac's electron zitterbewegung frequency $\omega_e = \frac{2m_e c^2}{\hbar}$. The pion cell size is $a_\pi = 7.757 * 10^{-15} \text{ meters}$. The pionic fabric density in free space is $\rho_{pion fabric} = \frac{1}{a_{pion cell}^3} = 2.1417 * 10^{42} \frac{pion cells}{m^3}$.

The classical and quantum hybrid quark molecular dynamics scheme for the pionic unit cell generates periodic trajectories shown below in figures 5 and 6. The distance between the four $\tilde{u}u$ and $\tilde{d}d$ quark pair of the pion cell are shown below and illustrate the active gluonic center (AGC) process where the quark exchanges occur vertically between \tilde{u} (1) and u (6) , \tilde{u} (5) and u (2) , \tilde{d} (3) and d (8) , \tilde{d} (7) and d (4) at the cusps.

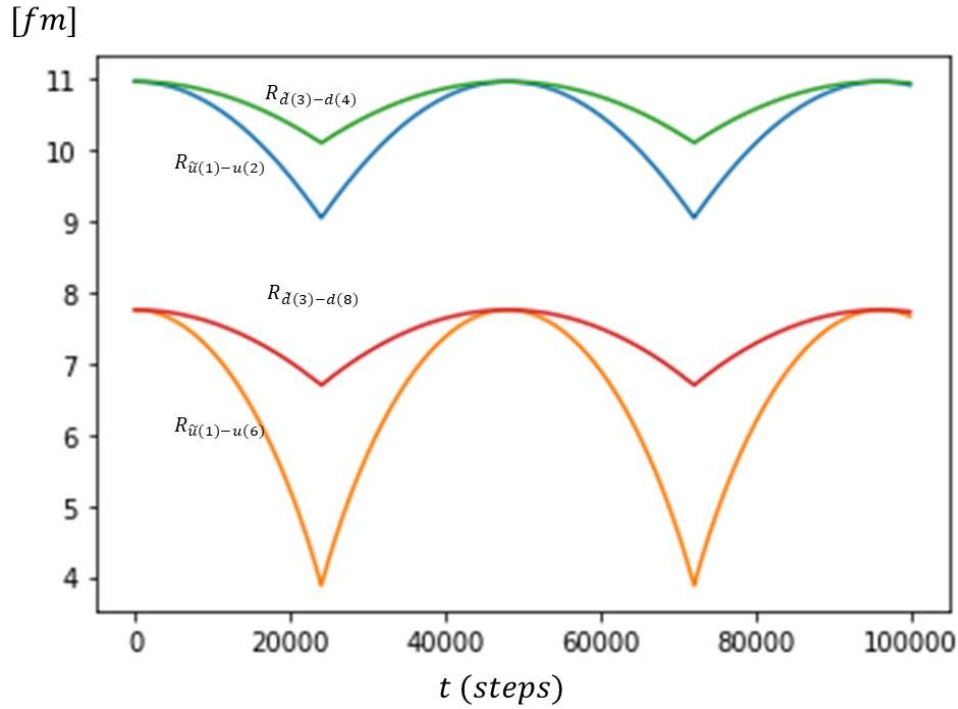


Figure 6 illustrates the quark and anti-quark pairs distances of the pion cell. The exchange operations occur at the cusps.

The potential and kinetic energies of the pionic fabric cell quarks and antiquarks are shown in figure 7. The pionic cell vibrates in and out towards the AGC. The quarks kinetic energy grows when the quarks fall in approaching the AGC and then is reduced gradually after the quark exchange occur at the cusps when the quarks move away from the AGC. We show that the total pion cell energy is zero, since there are infinite number of pion cells in the pionic fabric, their total energy remain 0. However, the pionic cells are not static and the quark dynamics is shown by the kinetic and potential energies of the pionic fabric unit cell in figure 7 analogues to a harmonic oscillator kinetic and potential energy.

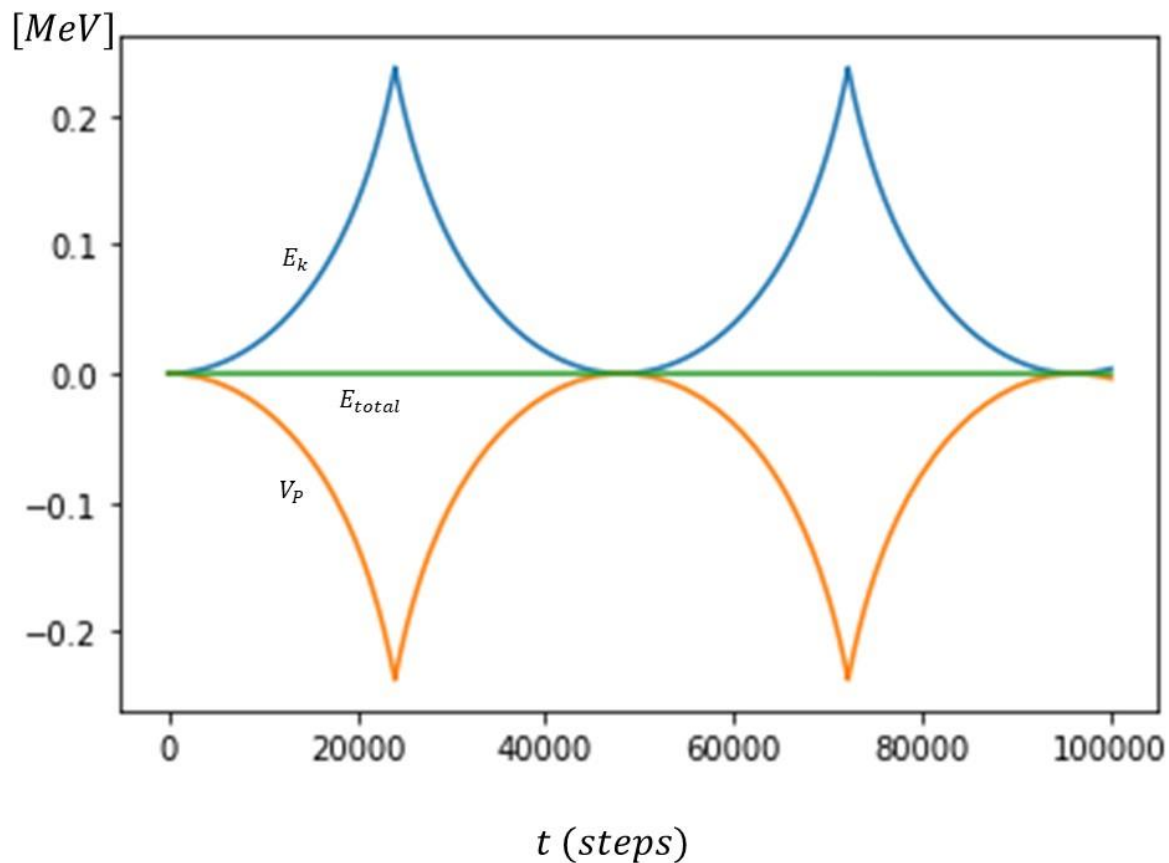


Figure 7 illustrates the zero-energy pionic fabric unit cell quarks and antiquarks oscillating potential and kinetic energies.

The X coordinate of the four quarks and anti-quarks of the first pion tetraquark, $\tilde{u}(1)$, $u(2)$, $\tilde{d}(3)$, $d(4)$ are shown below in figure 8 and the Z coordinate of $\tilde{u}(1)$ and $u(6)$ are shown in figure 9.

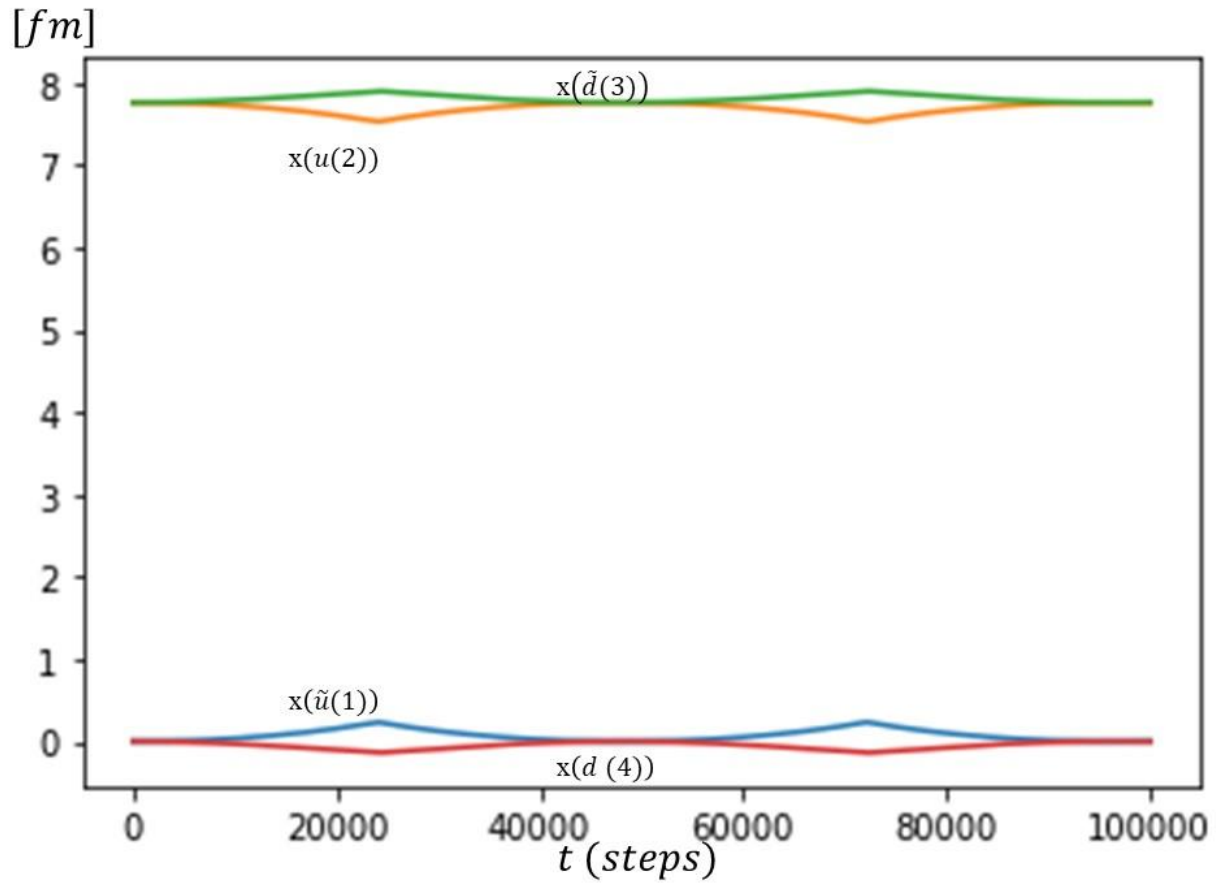


Figure 8 illustrates the X coordinate of the four quarks and anti-quarks of the first pion tetraquark.

The Z coordinate of $\tilde{u}(1)$ and $u(6)$ quarks performing the quark exchange at the AGC are shown below. The quark exchanges occur vertically between $\tilde{u}(5)$ and $u(2)$, $\tilde{d}(3)$ and $d(8)$, and $\tilde{d}(7)$ and $d(4)$ (not shown in the figure).

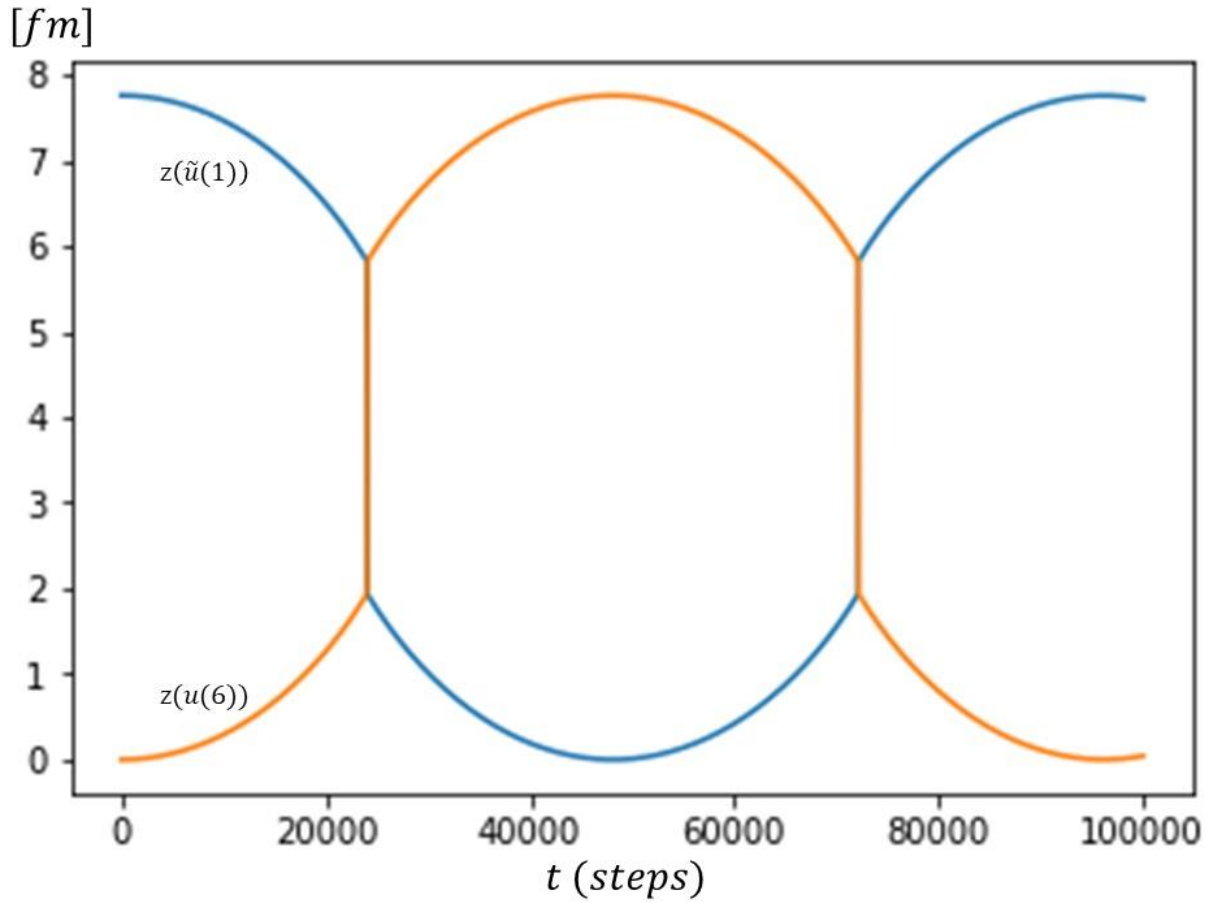
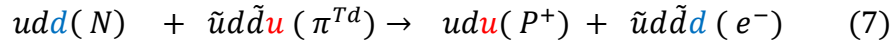


Figure 9 illustrates the Z coordinate of the $\tilde{u}(1)$ and $u(6)$ quarks.

5. The Electron and Pion Tetraquark Tetrahedron Cloud

Assuming that the β decay is a second order scattering reaction triggered by the vacuum pion tetraquark tetrahedrons¹⁰, the β decay generates a proton and a negatively charged exotic tetraquark, $\tilde{u}d\tilde{d}d$ that may be an electron tetraquark.



The reaction equation conserves quark number and flavor, and the exotic negatively charged tetraquark, $\tilde{u}d\tilde{d}d$, may be a non-elementary, non-point like electron. A first electron tetraquark state may be $\tilde{u}dd\tilde{d}$, and a second electron tetraquark state may be $\tilde{u}du\tilde{u}$ ¹⁰⁻¹⁴. Transforming an electron to a pion tetraquark tetrahedron in the pionic fabric may occur by quark exchanges between two adjacent fabric sites. A pion tetraquark tetrahedron may be transformed by a d and a u quark exchanges to an electron tetraquark tetrahedron and vice versa.

After the d and u quark exchanges, for example in vortex 2 of the pionic fabric unit cell shown in figures 4 and 5, the energy of the exchanged pionic unit cell is set to the electron rest mass energy of 0.511 MeV by contracting the pionic unit cell length by a factor of about 5 to the value $a_{pion\ cell} = 1.541 * 10^{-15}$ meters via setting the string tension parameter to a higher value $\sigma_{u,u} = 38$ KeV/fm.

Since the quark exchange reactions are symmetric, e.g. the reactants and products are identical as shown in equation 9 below, a double well potential model²³ may be used to represent the reaction like in ammonia molecule inversion²⁴. Accordingly, the motion of the electron tetraquark tetrahedron in the pionic fabric may occur via tunneling through double well potential barriers. The u and d quarks are exchanged as illustrated in figure 5 below. Note that the u and d quarks exchanges transfer a combined unit charge from the electron to the pion and vice versa.

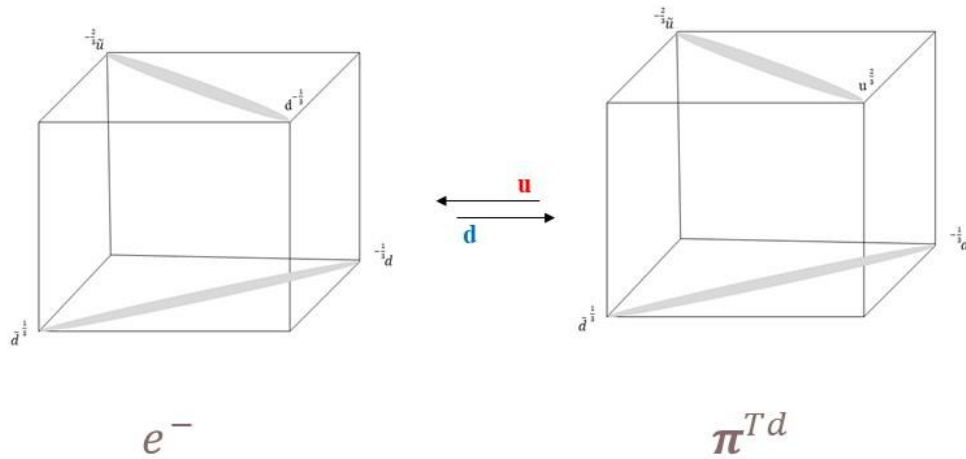


Figure 10 illustrates an electron tetraquark and a pion tetraquark tetrahedron exchanging quarks (u and d).

The Electron and Pion Tetraquark Tetrahedron Double Well Potential Model

The pion and electron quark exchange reaction between pionic fabric sites i and j are described in equation 9 where the d and the u quarks are exchanged. Since the reactants and products are identical a double well potential model is used below.

$$\tilde{u}d\tilde{d}d(e^L)_i + \tilde{u}d\tilde{d}u(\pi^{Td})_j \rightarrow \tilde{u}d\tilde{d}u(\pi^{Td})_i + \tilde{u}d\tilde{d}d(e^L)_j \quad (9)$$

In the case of the second electron exotic tetraquark state (R), the \tilde{u} and \tilde{d} antiquarks may be exchanged according to the following scattering reaction.

$$\tilde{u}d\tilde{d}u(\pi^{Td})_i + \tilde{u}d\tilde{u}u(e^R)_j \rightarrow \tilde{u}d\tilde{u}u(e^R)_i + \tilde{u}d\tilde{d}u(\pi^{Td})_j \quad (10)$$

A quantum mechanical solution for the double well potential model²³ is presented below and extended further to an electron and pion clouds:

$$\hat{H} = \frac{\hat{p}^2}{2m_e} + m_e \lambda (\hat{x}^2 - a^2)^2 \quad (11)$$

m_e is the electron rest mass, $2a$ is the distance between pionic fabric sites and the coupling parameter λ may be determined by the potential barrier height, $V_0 = m_e \lambda a^4$, where $V_0 = \hbar\omega_e = 2m_e c^2$. The frequency $\omega_e = \frac{2m_e c^2}{\hbar}$ is Dirac's free space trembling motion zitterbewegung frequency²⁸⁻²⁹.

Figure 11 below illustrates the double well potential for the electron tetraquark tetrahedron and the pion tetraquark tetrahedron quark exchange reaction in adjacent pionic fabric sites i and j . With the quantum mechanical double well potential model, the electron motion in the pionic fabric is via tunneling through the potential barrier V_0 . The barrier height $V_0 = 2m_e c^2$ is twice the electron rest mass energy, which is the threshold for electron-positron pair production. Note that the electron tetraquarks on both sides of the double well are identical and hence the electron state ($\tilde{u} dd\tilde{d}$ or $\tilde{u} du\tilde{u}$) is conserved.

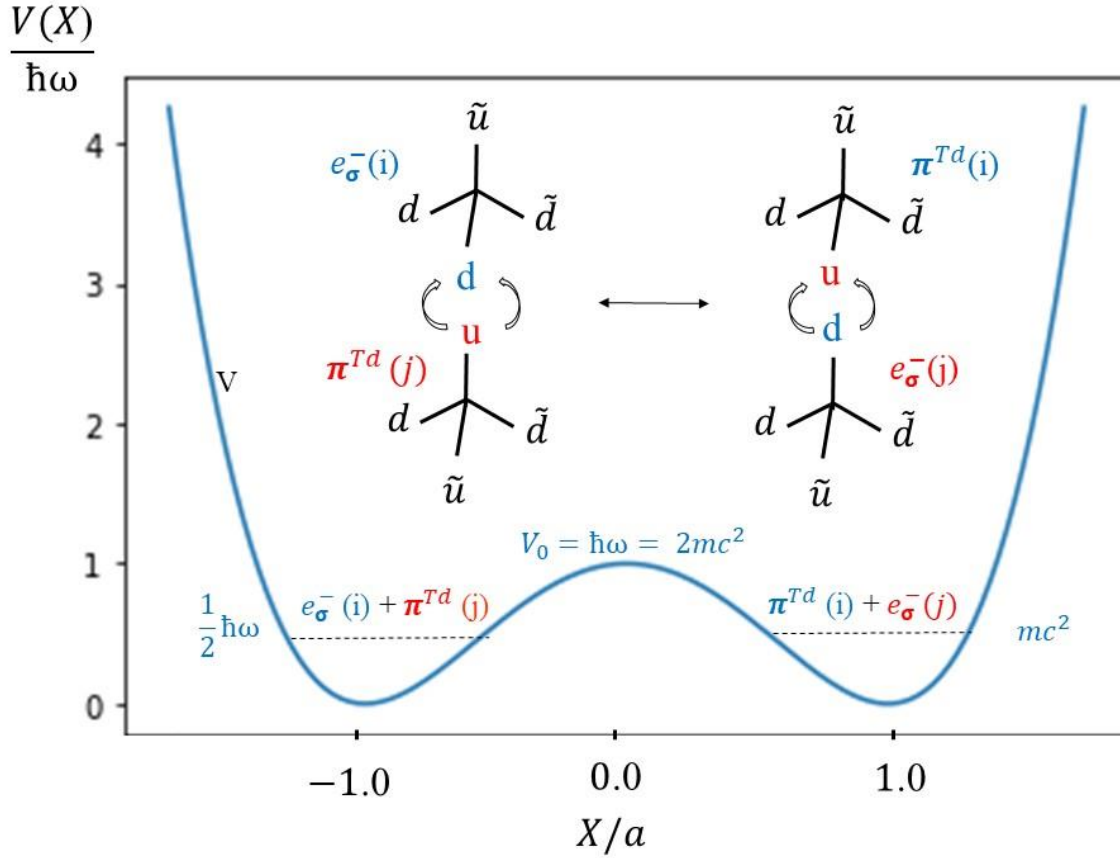


Figure 11 illustrates the double well potential model for the electron tetraquark tetrahedron and pion tetraquark tetrahedron quark exchange reaction in adjacent sites i and j in the pionic fabric.

The double well symmetric ground state and the antisymmetric first excited state energies and wavefunctions are calculated by diagonalizing the Hamiltonian (Eq. 11) using a Fourier plane wave basis set. The tunneling time, $T_{tunneling}$, from the left to the right potential well is an inverse function of the energy split between the first anti-symmetric state E_a and the symmetric ground state E_s . With the parameters above, $E_a = 1.0463 \hbar\omega$ which is just above the potential well barrier and $E_s = 0.7004 \hbar\omega$ is a bound state inside the potential well. The tunneling time is $5.849 * 10^{-21}$ seconds.

$$T_{tunneling} = \frac{\pi\hbar}{E_a - E_s} = 5.849 * 10^{-21} \text{ seconds} \quad (12)$$

A superposition of the symmetric and antisymmetric eigenstates is taken as the initial state $\psi_{t=0}$ describing an electron wavepacket located in the left well initially.

$$\psi_0 = \frac{1}{\sqrt{2}} (\psi_s + j \psi_a) \quad (13)$$

After half a period the electron wavepacket tunnels to the right well

$$\psi_{T_p/2} = \frac{1}{\sqrt{2}} (\psi_s e^{-iE_s T_p/2} + j \psi_a e^{-iE_a T_p/2}) \quad (14)$$

The electron wavepacket continues oscillating between the two wells with a period of $T_p = \frac{2\pi\hbar}{E_a - E_s}$.

The electron velocity in the pionic fabric may be calculated by dividing the distance between two adjacent wells, $2a$, by the tunneling time.

$$v_e = \frac{2a}{T_{tunneling}} = \frac{2a(E_a - E_s)}{\pi\hbar} = 0.44 c \left[\frac{m}{sec} \right] \quad (15)$$

Note that the electron velocity here is about half of the speed of light and that the tunneling frequency is on the time scale of the free space trembling motion zitterbewegung frequency, similar to semi-classical electron models²⁵⁻²⁶.

6. The Electron and Pion Tetraquark Tetrahedron Cloud

The single electron and pion tetraquark tetrahedron double well potential model can be extended to the pionic fabric where the electron with the pionic fabric tetrahedrons are assumed to form a dense and polarized sphere. In the center of the sphere, the double well potential model length may be extremely small below the Compton length. Away from the cloud center, the distance between pion tetraquark tetrahedron cells may increase. After about few Compton lengths, the distance between pion cells is such that the quark exchange reactions stop. The electron tunneling exponentially decreases and the electron is trapped in the pion cloud sphere by the lack

of quark exchange reactions outside the sphere. The electron is confined by the pionic fabric sphere that forms the electron cloud.

The following table summarizes the two lower energy eigenvalues with increasing distance between the two potential wells, $2a$, $4a$ and $6a$ keeping the potential barrier height at the same value, $V_0 = 2m_e c^2$, by changing the value of the coupling parameter λ , $\lambda = \frac{2c^2}{a^4}$, $\lambda = \frac{2c^2}{16a^4}$ and

$$\lambda = \frac{2c^2}{81a^4}.$$

Distance between the two wells	$E_a/\hbar\omega$	$E_s/\hbar\omega$	$T_{tunneling}(\text{sec})$
$2a$	1.0463	0.7004	5.849510^{-21}
$4a$	0.4741	0.4502	8.457710^{-20}
$6a$	0.318497	0.31698	1.34040^{-18}

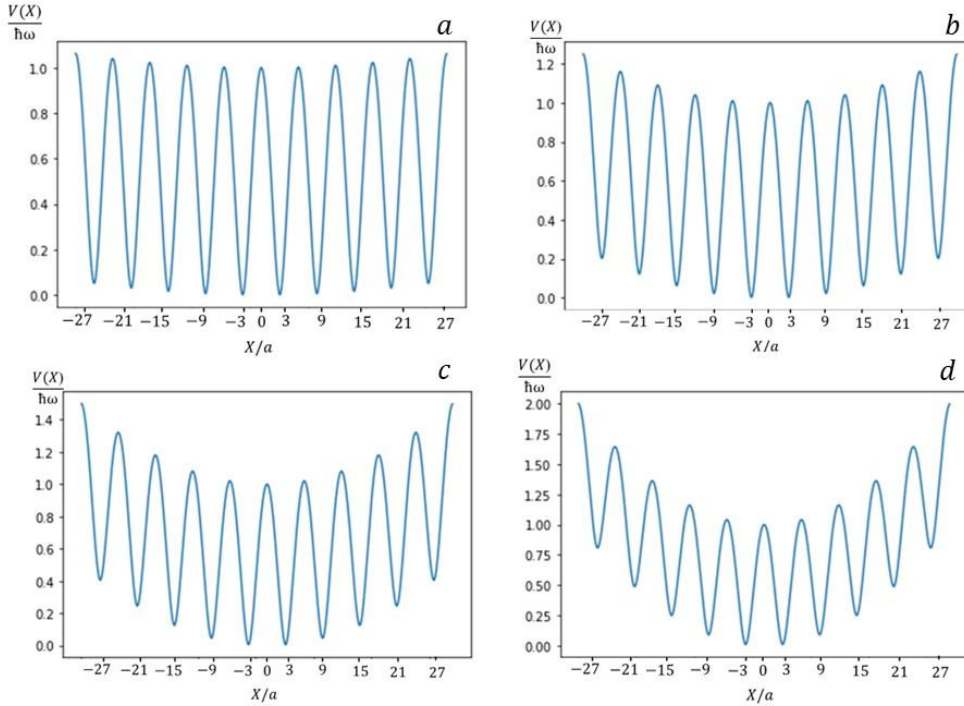
The electron tunneling time between the two wells is reduced significantly with the growth of the distance between the wells. With the $6a$ distance the tunneling is about 229 times slower than with $2a$ distance (a is defined as the electron Compton length $\frac{\hbar}{m_e c}$). The extremely fast electron wavepacket dynamics in the pionic fabric may be observed in the future with the new attosecond electron microscopy²⁷.

The pionic fabric cell length in free space, far from any charged or massive body at ∞ is $a_\pi = 7.757 \cdot 10^{-15}$ meters and after the d quark exchange the u quark charging the pionic cell, the charged pionic cell length contracts by a factor of 5, $a_{pionic\ cell}(embedded\ electron) = 1.541 \cdot 10^{-15}$ meters and hence the pionic density in the electron cloud becomes much higher than in free space,

$$\rho_{\text{pion fabric}}(\text{embedded electron}) = \frac{1}{a_{\text{pion cell}}^3(\text{embedded electron})} = 2.73 * 10^{44} \frac{\text{pion cells}}{\text{m}^3}.$$

The embedded electron charge polarizes the pionic fabric in a sphere around the electron since the pionic fabric cells have built in electric dipole moments and also since the rapid quark exchanges moves the electron from site to site rapidly. We assume that the polarization of the pionic fabric cloud due to the electron adds a long-range harmonic potential term $\sim \frac{\hbar\omega x^2}{L^2}$, where L is the length scale of the pionic fabric cloud sphere.

The electron and pion tetraquark tetrahedron potential is extended in one dimension with 10 pionic fabric sites and with increasing long-range harmonic potential term, 0.25, 1, 2 and 4 $\frac{\hbar\omega x^2}{L^2}$ for the pion cloud model.



Figures 8a-d illustrates the electron and pion tetraquark tetrahedron cloud potential in one dimension with 10 fabric sites and increasing long- range harmonic potential term ((a) 0.25, (b) 1, (c) 2 and (d) 4 $\frac{\hbar\omega x^2}{L^2}$).

The two lowest symmetric, ψ_1 , and antisymmetric, ψ_2 , eigenfunctions are shown below for the four long-range harmonic potential values. Note that the eigenfunctions peaks are localized in the pionic fabric wells and that in the two lower states, the tetraquark electron is not localized in a single well, it has a finite probability to be found in few adjacent wells in the pionic fabric.

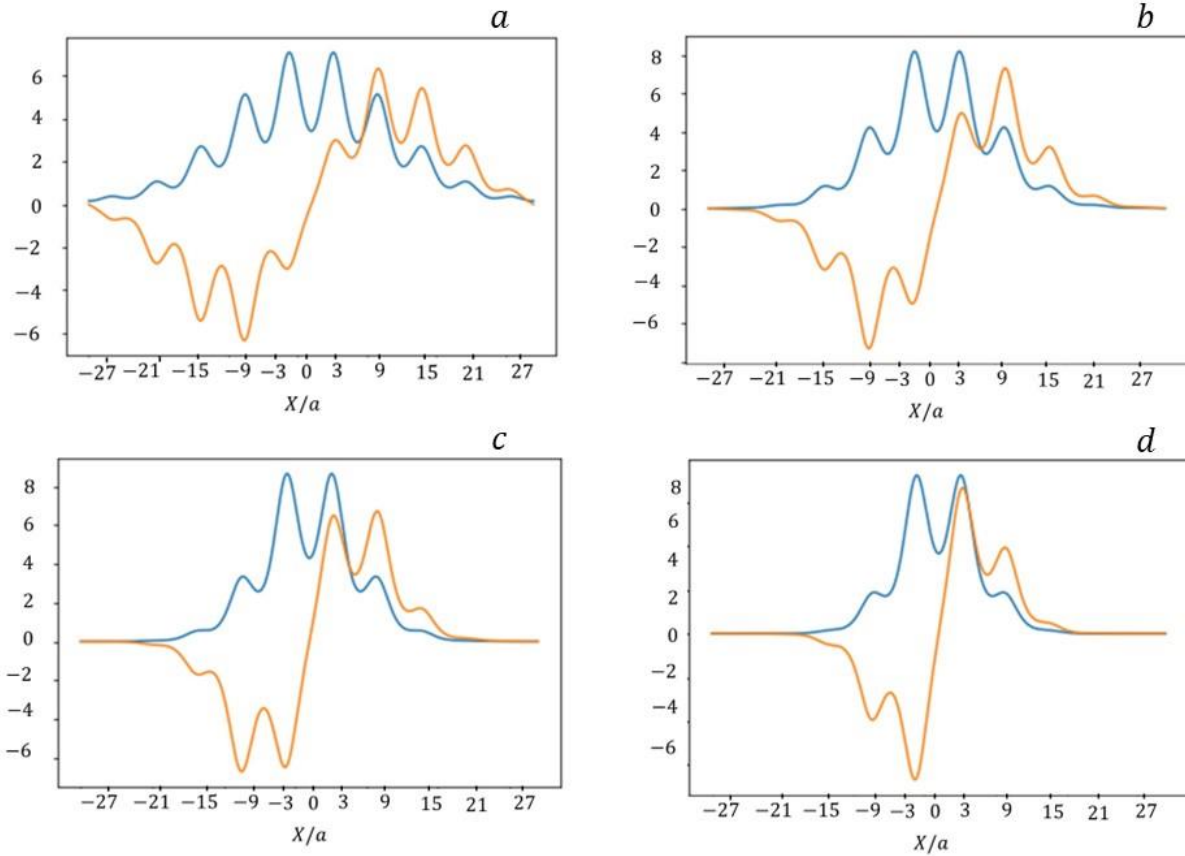


Figure 9a-d illustrates the first and second symmetric ψ_1 and antisymmetric ψ_2 eigenfunctions for the four long-range harmonic potential values ((a) 0.25, (b) 1, (c) 2 and (d) $4 \frac{\hbar\omega x^2}{L^2}$).

An initial wavepacket can be formed by a superposition of the two lower symmetric and antisymmetric eigenstates, $\psi_0 = \frac{1}{\sqrt{2}} (\psi_1 + j\psi_2)$. The electron wavepacket has high probability to be found in the first few wells on the left initially. After half a period, the wavepacket tunnels to

the right-hand side wells (in blue). Note that with higher value of the long-range harmonic potential the low eigenstates are localized mainly in a single pionic fabric site as shown in figures 10d.

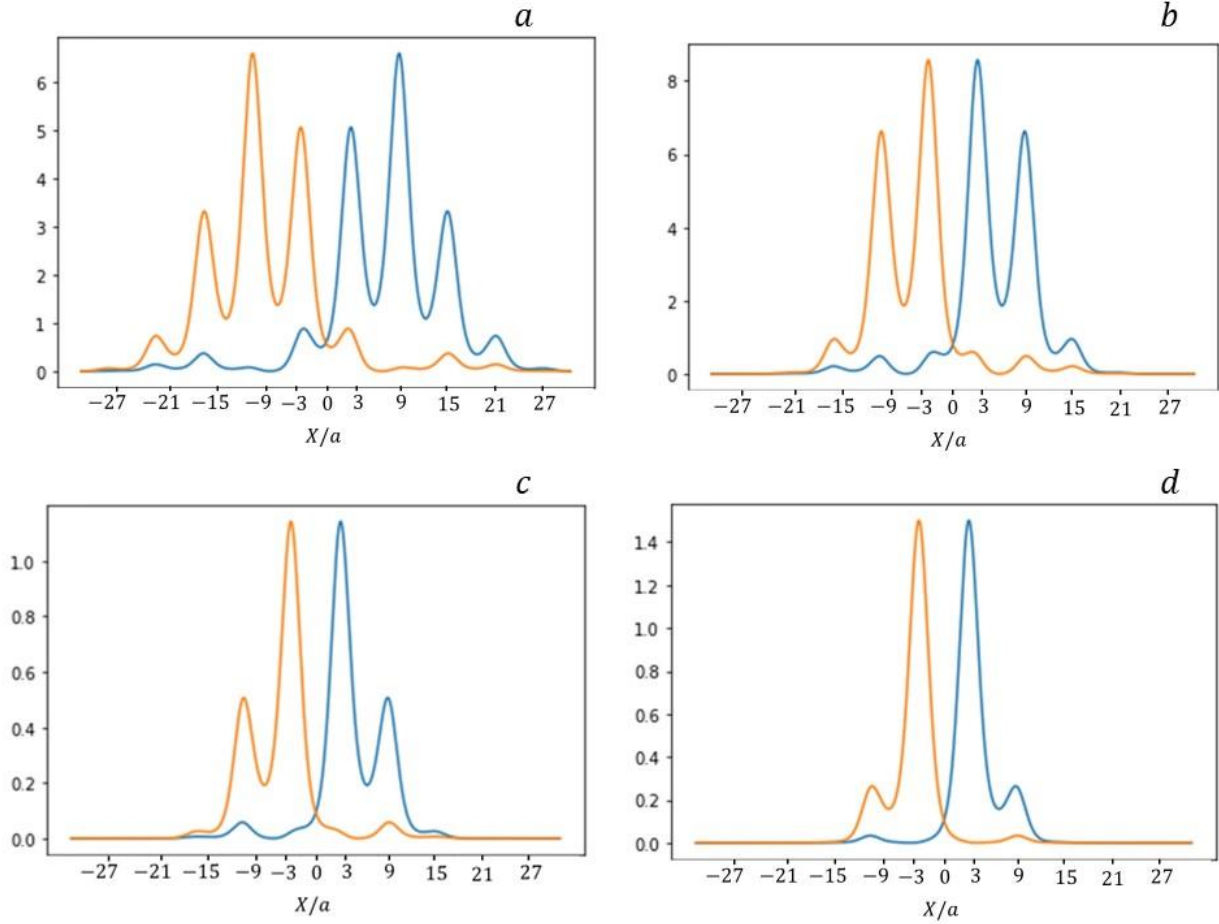


Figure 10a-d illustrates the electron wavepacket at $t=0$ (in orange) and after a half time period (in blue) for the four long -range harmonic potential values ((a) 0.25, (b) 1, (c) 2 and (d) $4 \frac{\hbar\omega x^2}{L^2}$).

The position expectation value of the electron wavepacket for 5 time periods for the four long-range harmonic potential values calculated according to equation 16 are shown in figures 11a-d.

$$X(t) = \langle \psi_t | \hat{X} | \psi_t \rangle \quad (16)$$

The position expectation value oscillates between the left-hand side wells to the right-hand side wells. With higher long-range harmonic potential value the oscillation amplitude decreases since the wavepackets are more localized in the first wells.

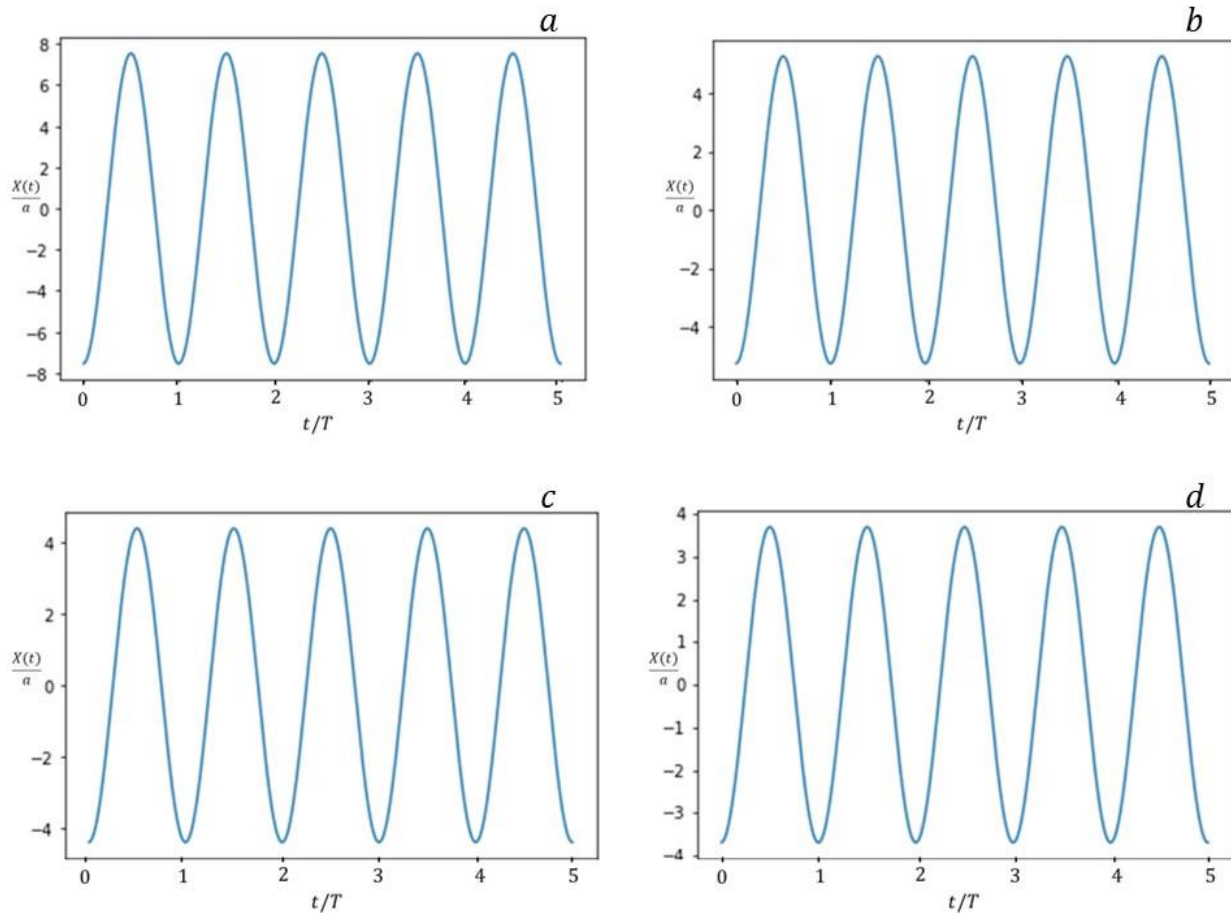


Figure 11a-d illustrates the position expectation value of the electron wavepacket for 5 time periods for the four long -range harmonic potential values ((a) 0.25, (b) 1, (c) 2 and (d) $4 \frac{\hbar\omega x^2}{L^2}$).

The higher symmetric ψ_7 and antisymmetric ψ_8 eigenstates are localized in the outer wells. The superposition, $\psi_0 = \frac{1}{\sqrt{2}} (\psi_7 + j\psi_8)$, is shown below where the tunneling occurs now between the outer wells.

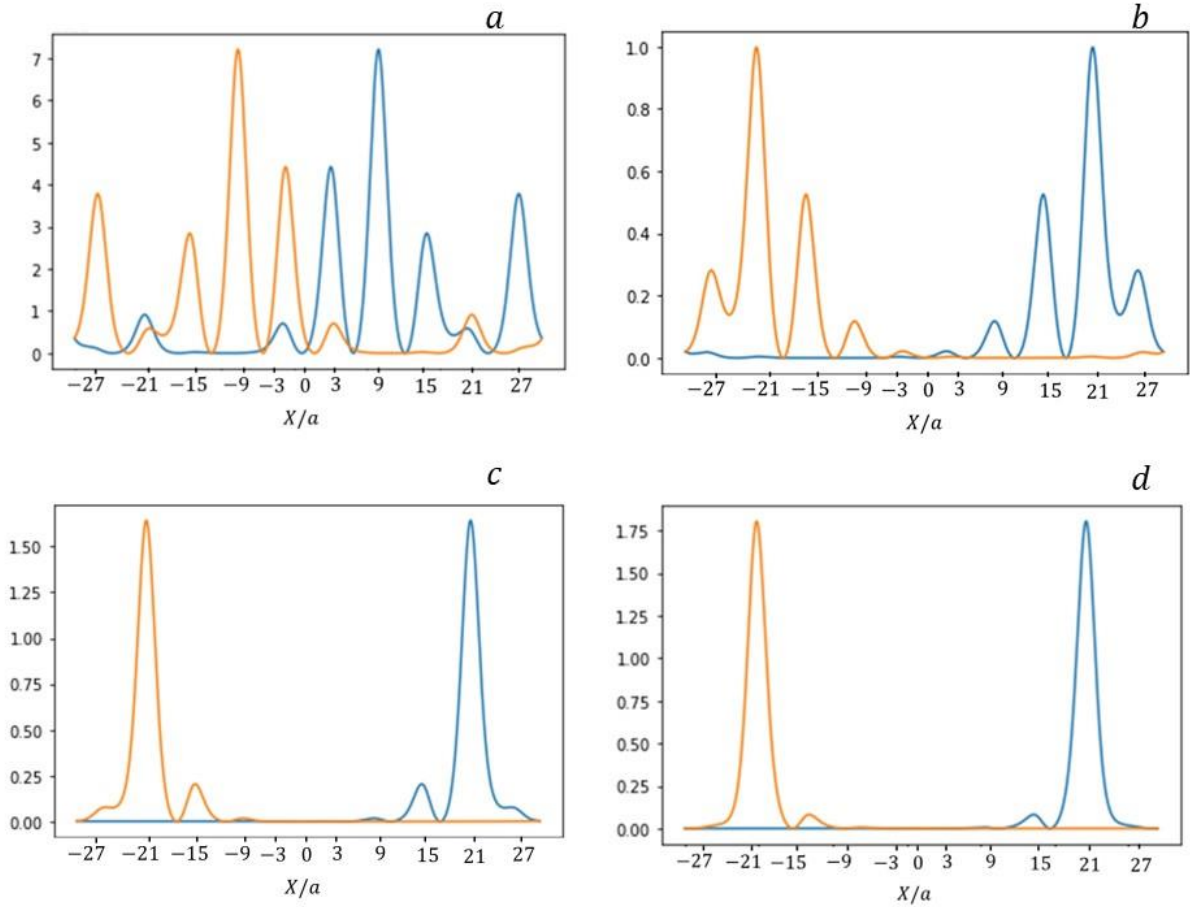


Figure 12a-d illustrates the electron wavepacket at $t=0$ (in orange) and after half time period (in blue) for the four long-range harmonic potential values ((a) 0.25, (b) 1, (c) 2 and (d) $4 \frac{\hbar\omega x^2}{L^2}$).

We assume that the polarization effect of the charged electron on the pionic fabric is to rearrange the pionic fabric sphere with the speed of light around the electron site. The length parameter a may be changed numerically ($\sim 0.46 \frac{\hbar}{m_e c}$ for example) such that the calculated electron velocity according to equation 11, $v_e = \frac{2a(E_a - E_s)}{\pi\hbar}$, will be close to the speed of light. In this case, the rearrangement of the pion tetrahedrons cloud and the tunneling of the electron wavepacket occurs at maximal speed and the electron speed is limited to c since the pionic fabric cannot rearrange faster.

The electron tunnels from site to site in the pionic fabric extremely fast with the zitterbewegung frequency and it cannot be isolated as a single particle. Note that the vibration frequency of the quarks of the pionic fabric is equal to the electron zitterbewegung frequency. The motion of the electron in the pionic fabric cloud is in resonance with the pionic fabric oscillations. Schrödinger suggested that the electron particles would be described with wavepackets and found that a Gaussian wavepacket formed by a linear combination of plane waves gets wider linearly with time in free space¹. The electron wavepacket simulations above do not prove the proposed quark model of the electron and pionic fabric but it does show that a confined electron wavepacket may be obtained with a pionic fabric cloud. Lattice QCD may allow calculating the mass of the electron and pionic fabric unit cell and support the proposed quark model of the electron and the pionic fabric. With the proposed model, the electron is not bare like Dirac assumed. The perturbative free particle bare propagator may be the cause for the divergence of the vacuum polarization and electron self-energy Feynman integrals²⁸⁻³⁰. The pionic fabric may overcome these divergencies that may be mathematical only and not physical.

7. The Positron Tetraquark Tetrahedron

The positron tetraquark tetrahedrons have a positive charge of the u and \tilde{d} quarks replacing the negative charge of a \tilde{u} and d quarks of the electron tetraquark tetrahedrons as shown below in figures 13 (a-b) for the electrons on the left and for the positrons on the right in figures 13 (c-d). Two positron enantiomers, e_R^+ and e_L^+ , may exist like the two electron enantiomers e_R^- and e_L^- . In the four cases, quark exchanges transform the electrons, or the positrons, to a pion tetraquark tetrahedron (π^{Td}) and vice versa conserving charge and the electron/positron tetraquark state.

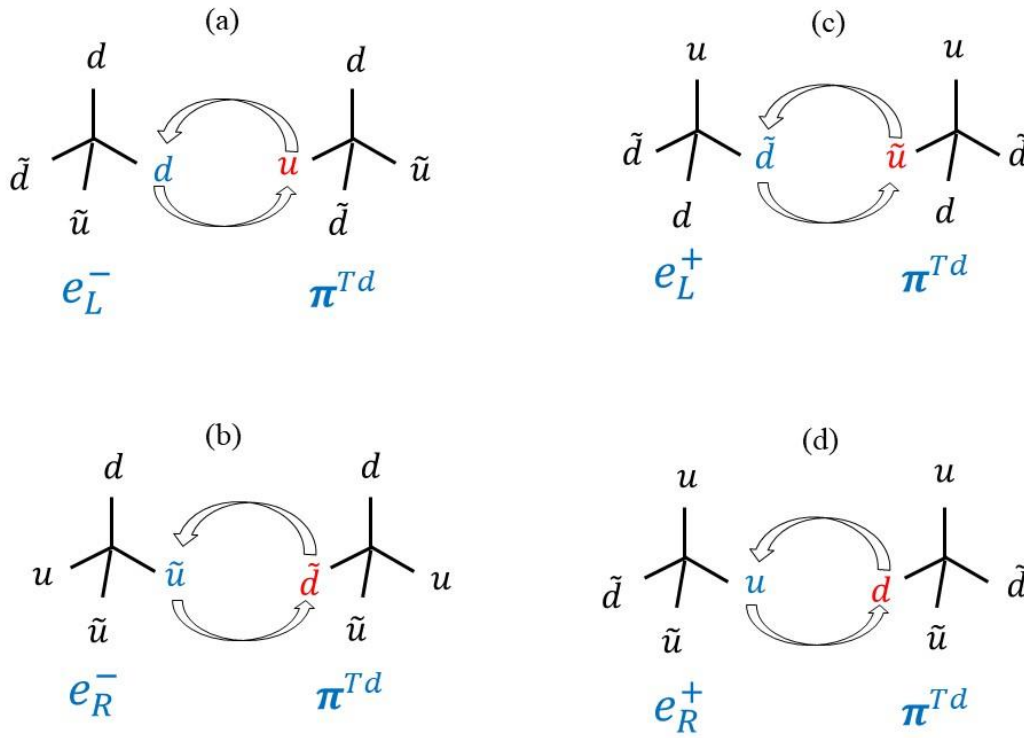


Figure 13 illustrates electron tetraquark tetrahedron enantiomers (a) and (b) and positron tetraquark tetrahedron enantiomers (c) and (d) exchanging quarks with pion tetraquark tetrahedrons with symmetric reactions such that the electrons and positrons transform to pion tetraquark tetrahedrons and vice versa conserving charge and the electron/positron tetraquark state.

8. Electron-Positron Creation and Annihilation in the pionic fabric

Electron-positron annihilation in the pionic fabric may occur by a u and d quark exchanges of an electron tetraquark tetrahedron and a positron tetraquark tetrahedron forming two neutral pion tetraquark tetrahedrons that become part of the pionic fabric as shown in equation 17.



An electron tetrahedron in site i in the fabric collides with a positron tetraquark in adjacent site j and the outcome is that both sites after the collision will have pions, where the electron and positron charges and spins are annihilated. The extra energy of the electron and positron may be

transferred to the pionic fabric as electromagnetic wave energy. Note that in equation 17 the number and flavor of the quarks are conserved. The quarks are not destroyed nor created in the quark exchanges¹⁰⁻¹⁴.

Electron-positron creation may occur in a pionic fabric cell where a u quark in vortex 4 exchange positions with a d quark in vortex 2 as shown below. The outcome of the quark exchanges is that on the right-hand side of the pionic fabric cell an electron tetraquark ($\tilde{u}dd\tilde{d}$) is created and on the left-hand side of the pion cell a positron tetraquark ($u\tilde{u}u\tilde{u}$) is created. The electron-positron pair can next split and propagate in the pionic fabric or re-combine by exchanging back the u and d quarks forming a neutral pionic fabric cell.

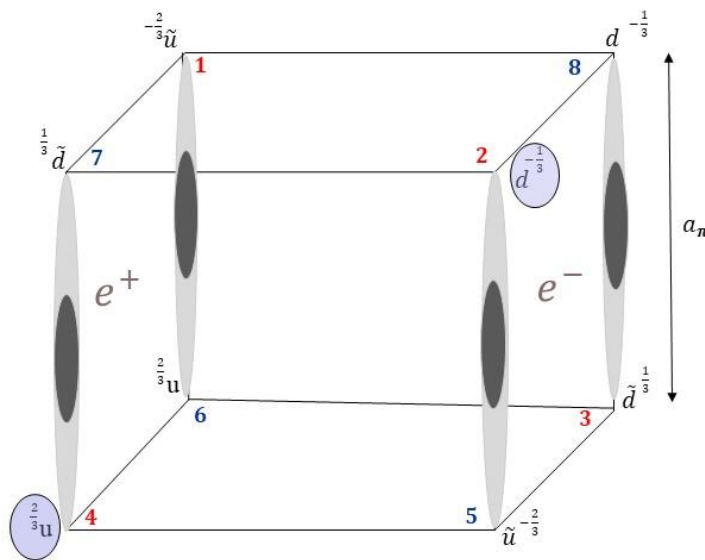


Figure 14 illustrates the pionic fabric cubic unit cell with an exchange of a d and a u quark in vertices 2 and 4 that create an electron-positron pair ($u\tilde{u}u\tilde{u}$ (e^+) and $\tilde{u}dd\tilde{d}$ (e^-)).

9. The Proton and the Pionic fabric

Protons and neutrons can be embedded and confined in pionic fabric cells. The existence of the three proton quarks in the pionic fabric cell contracts the cell length to sub-femtometers. With string tension $\sigma_{u,u}$ of 7.6 GeV/ femtometer, the pionic cell length of the embedded proton is $0.0648 * 10^{-15}$ meters such that the embedded proton pionic cell energy is equal to the rest mass of the proton of 936.38 MeV. The embedded proton pionic cell length is shorter by a factor of about 120 comparing to the free space pionic cell of $7.757 * 10^{-15}$ meters calculated with equations 7-10 above.

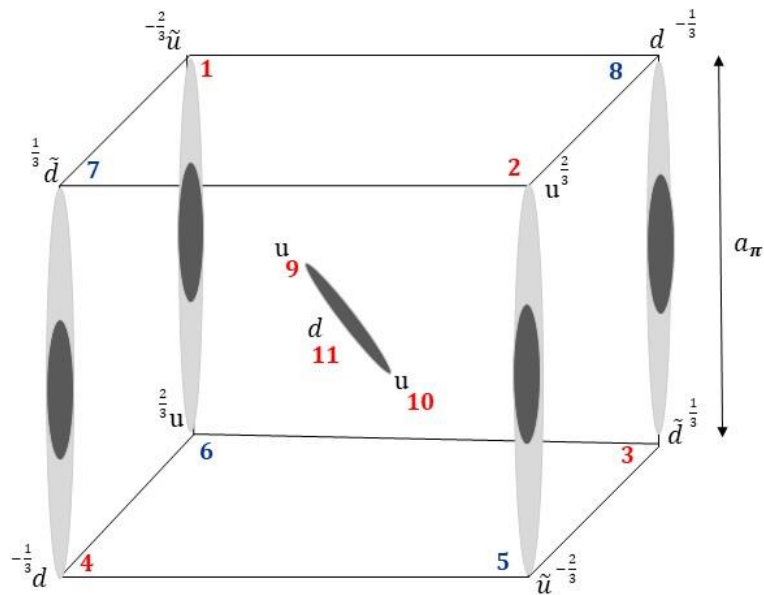


Figure 15 illustrates the embedded proton in the pionic cell tilted along the cell diagonal.

The proton is positioned at the pion cell center and is tilted along the cell diagonal towards the two \tilde{u} quarks at corners 1 and 5 above. The proton two u quarks are separated by the d quark positioned at the cell center. The two u quarks are attracted to the d quark negative charge and they perform quark position exchanges and velocities flip at the AGC surface at a distance of about 0.00076 femtometers that prevent the u quarks fall into the coulomb singularity at $r_{u,d} \rightarrow 0$. The Z coordinate of the pion cell \tilde{u}_1 antiquark and u_6 quark and the proton quarks u_9 and u_{10} are shown in the figure below. On the pion cell scale, the vibration motion of the quarks is small.

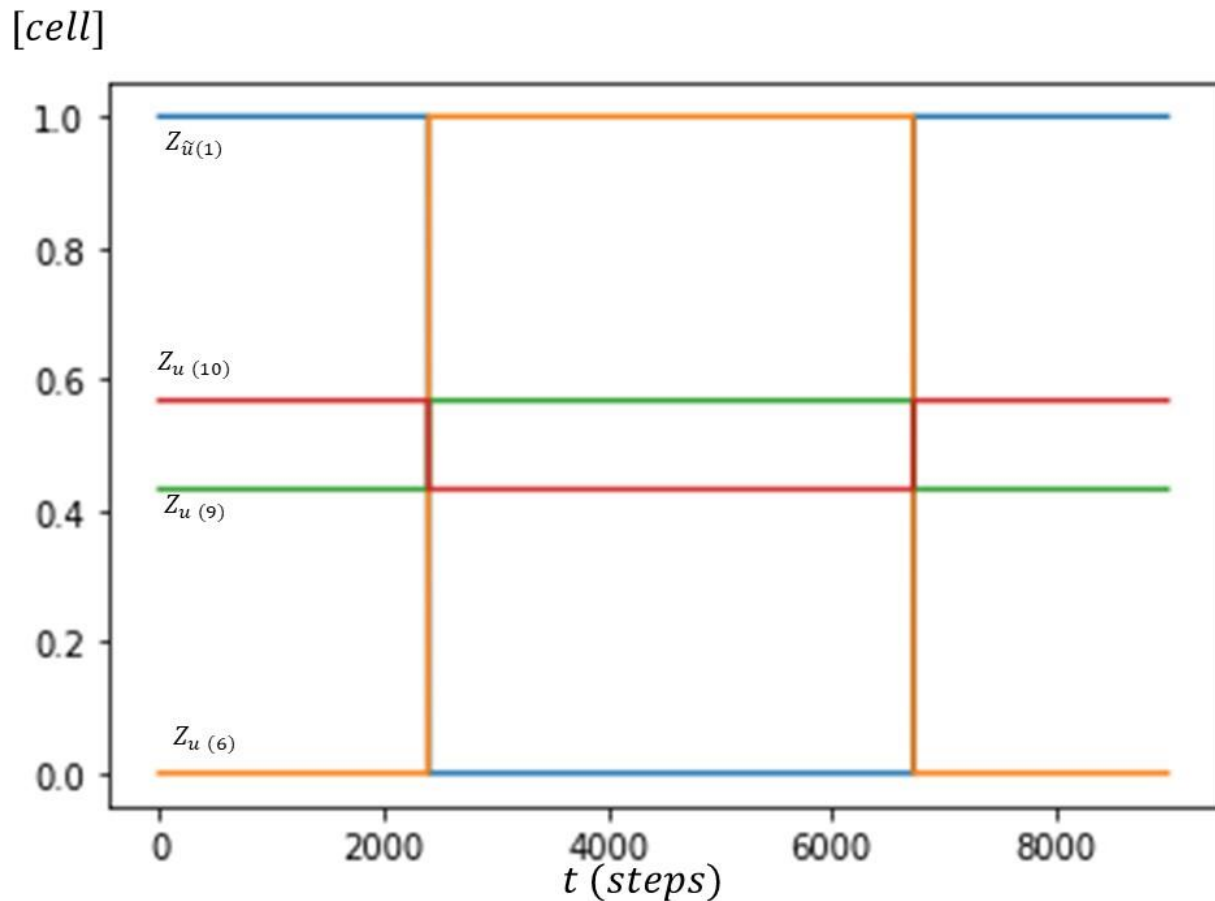


Figure 16 illustrates the Z coordinate of the pion cell \tilde{u}_1 antiquark and u_6 quark and the proton quarks u_9 and u_{10} in the embedded proton pionic cell.

Figure 17 illustrates the energy of the proton and pion cell during two quark exchange operations. Since the pion cell symmetry is different than the proton inversion symmetry, the exchange of the pion quarks and antiquarks, \tilde{u}_1 and u_6 , \tilde{u}_5 and u_2 , \tilde{d}_3 and d_8 , \tilde{d}_7 and d_4 , and the proton quarks u_9 and u_{10} changes the potential energy of the quarks. The second quark and antiquark exchange changes the potential energy back to the first configuration and hence the energy first grows and then is reduced back as shown below. The energy changes may be seen as energy transfer between the proton quarks and the pionic fabric quarks.

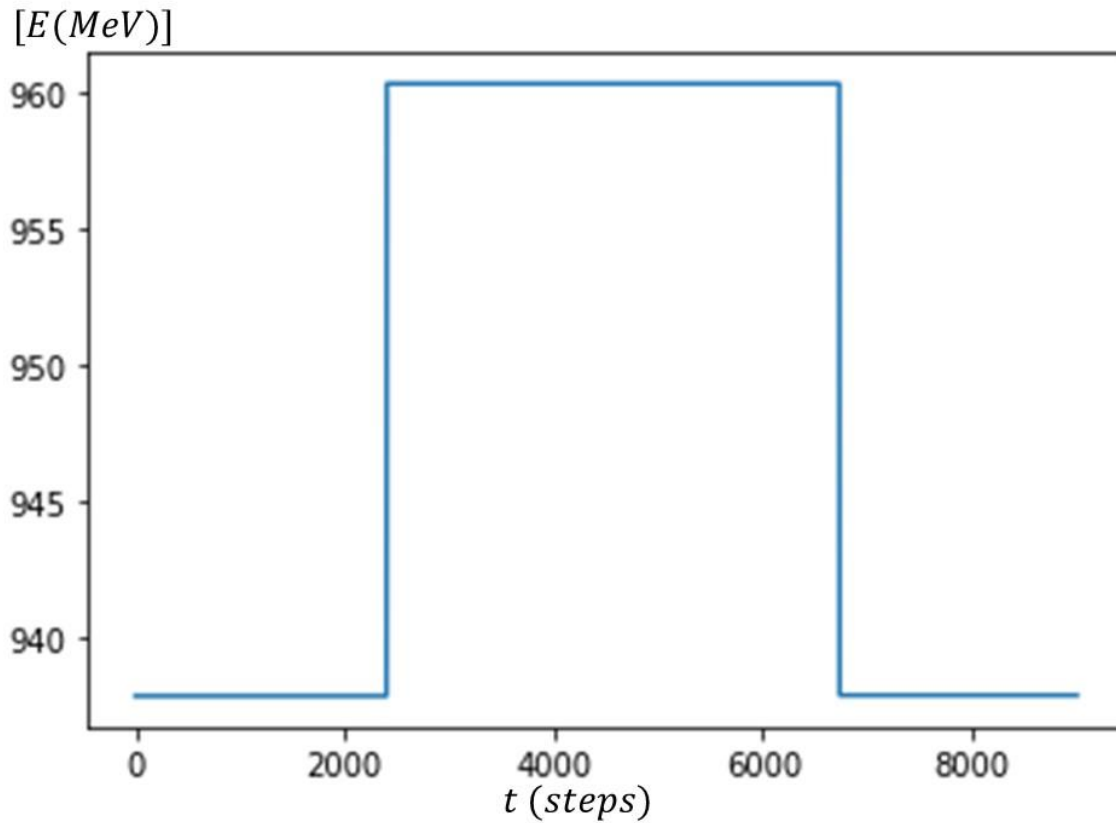


Figure 17 illustrates the energy of the proton and pion cell during two quark exchange operations.

Figure 18 illustrates the distance between the proton u_9 and u_{10} quarks during the trajectory with two exchange operations at the pion cell AGC. After the first quark exchange operation, the two quarks see different quark configuration of the pion cell since each quark is replaced with its antiquark and hence the fall and the bounce back is not fully symmetric. The second bounce at the AGC exchanges back the pion quarks to their first configuration and then the proton quarks trajectory follows the opposite path that preceded the first bounce as shown below.

[fm]

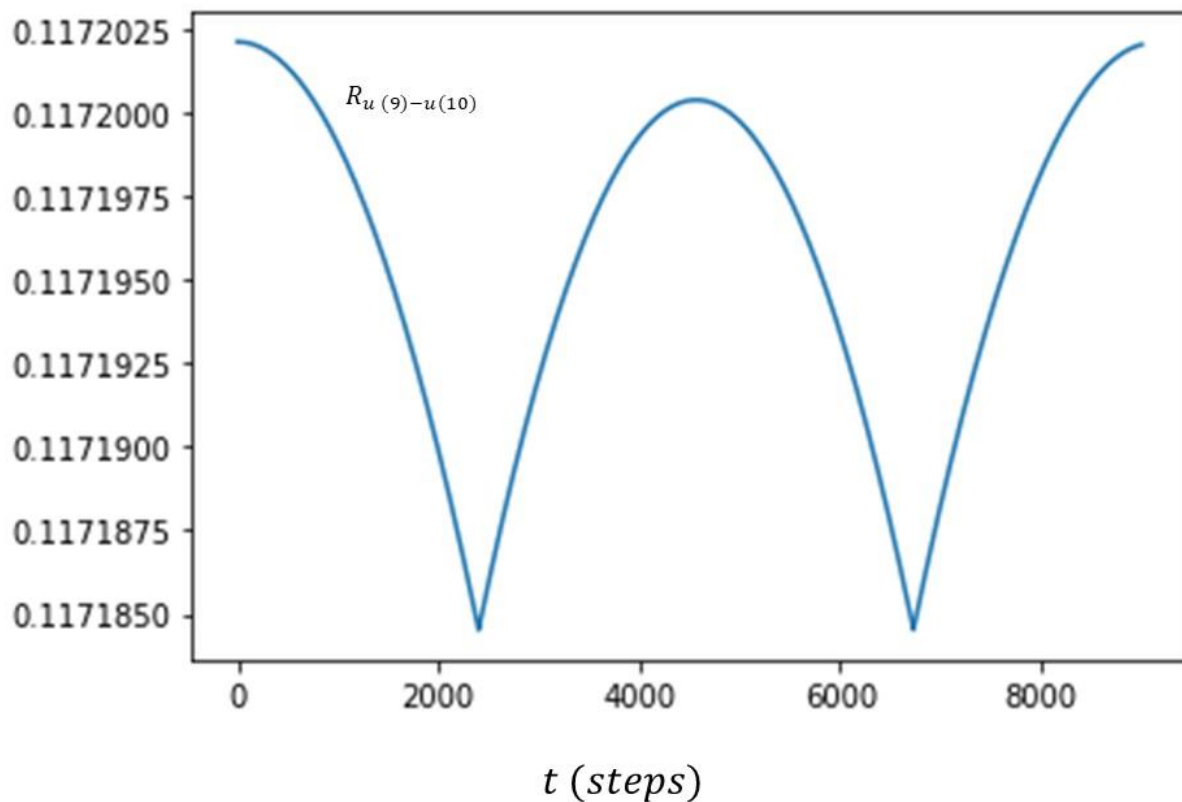


Figure 18 illustrates the distance between the proton quarks u_9 and u_{10} with the two exchange operations at the cusps.

The Pionic Fabric Density Around Charged and Massive Bodies Model

In the vicinity of massive bodies, the pionic fabric and pionic cells may be curved and may have a spherical symmetry where the pionic cells are forced to reshape and fill a sphere for example. Near a black hole, the pionic fabric cells may be extremely curved and dense, where far away in space in cosmic voids³¹⁻³³, the pionic fabric cells may be diluted and have cubic cells in flat space.

In the case of a Hydrogen atom, the pionic fabric density grows from the free/flat space value of $\rho_{pion\ fabric}(\infty) = 2.73 * 10^{44} \frac{pion\ cells}{m^3}$, to a significantly higher density in the vicinity of the embedded proton. The embedded proton pion cell length is $0.0648 * 10^{-15}$ meters, two orders of magnitude smaller than the pion cell length in free space of $7.757 * 10^{-15}$ meter. We can model the pionic fabric density in the vicinity of the proton at radius r using the pionic fabric unit cell length far from the proton in free space and at the proton site using an exponential fall with a parameter λ_p that we will determine next.

$$\rho_{pion\ fabric}(r - r_p) = \frac{1}{a_{pion\ cell}^3(\infty)} + \frac{e^{-(r-r_p)/\lambda_p}}{a_{pion\ cell}^3(embeded\ proton)} \quad (18)$$

Note that in analogy to the exponential fall of the atmospheric density with elevation from earth¹⁰, the pionic fabric density falls exponentially with distance from the embedded proton and the density gradient will affect the dynamics of particles in the pionic fabric. For example, the motion of the electron tetrahedron in the fabric via u and d quark exchanges will be sensitive to the fabric density variations since it will change the tunneling rates via the pionic fabric cells and potential barriers. The electron and pion cloud may be confined by the pionic fabric curvature and density variations due to the embedded proton pionic cell.

Using the quark molecular dynamics scheme we calculated the embedded proton pionic cell length $a_{pionic\ cell}(embedded\ proton) = 0.0648 * 10^{-15}$, the electron pionic cell length $a_{pionic\ cell}(embedded\ electron) = 1.541 * 10^{-15}$ meters, and the free space pionic fabric cell length $a_{pionic\ cell}(\infty) = 7.757 * 10^{-15}$ meters. The pionic fabric density exponential fall parameter λ_p can be calculated using the three densities' values. Assuming that for the Hydrogen atom at a distance of the Bohr radius, $a_{Bohr} = 0.523 * 10^{-10}$ meters, the pionic fabric cell density is –

$$\rho_{pion\ fabric}(embedded\ electron) = \frac{1}{a_{pion\ cell}^3(embedded\ electron)} = 2.73 * 10^{44} \frac{pion\ cells}{m^3} \quad (19)$$

Next using equation 18 and 19, we derive the expression for λ_p -

$$\rho_{pion\ fabric}(a_{Bohr}) = \frac{1}{a_{pion\ cell}^3(\infty)} + \frac{e^{-a_{Bohr}/\lambda_p}}{a_{pion\ cell}^3(proton)} = 2.73 * 10^{44} \frac{pion\ cells}{m^3} \quad (20)$$

$$\lambda_p = \frac{-a_{Bohr}}{\ln\left(\frac{a_{pion\ cell}^{-3}(embedded\ electron) - a_{pion\ cell}^{-3}(\infty)}{a_{pion\ cell}^{-3}(embedded\ proton)}\right)} = 0.0559 * 10^{-10} m \quad (21)$$

λ_p is one order of magnitude smaller than the Bohr radius, however, as shown below, the pionic fabric density at the Hydrogen atom Bohr radius is about 120 times higher than in free space and it grows exponentially closer to the embedded proton pionic cell.

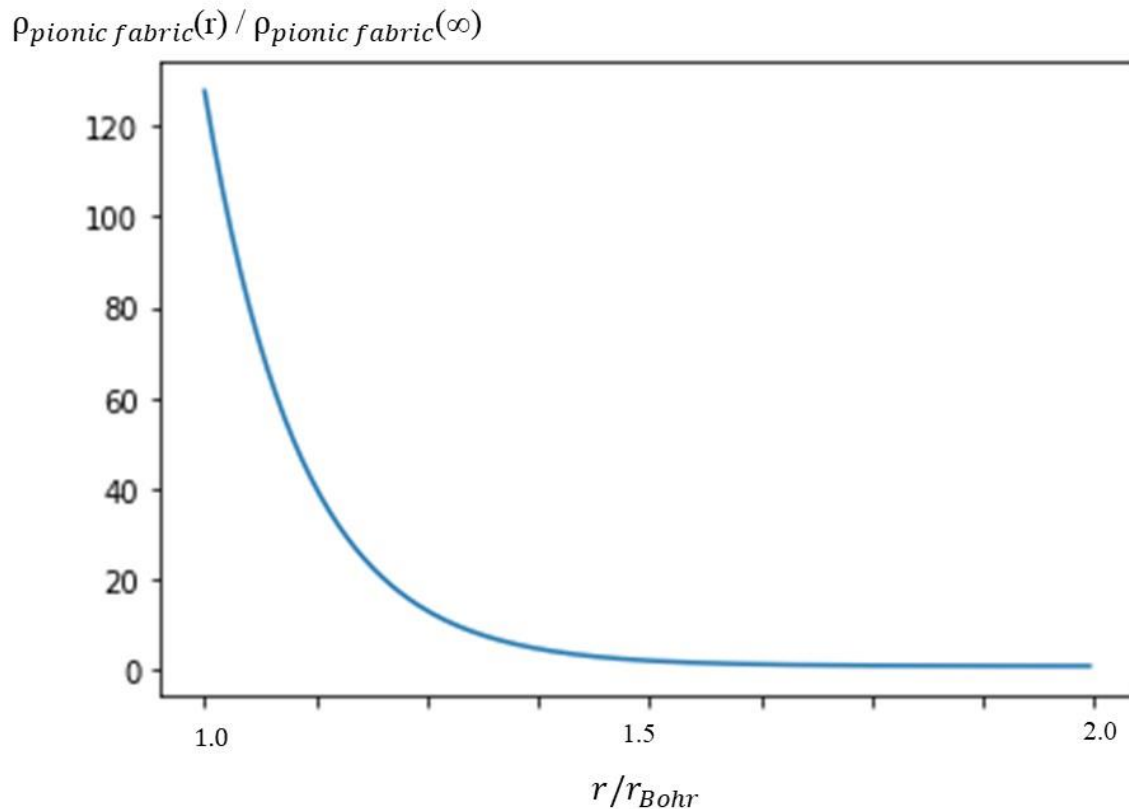
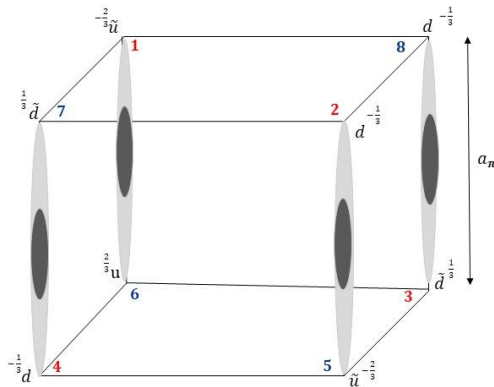


Figure 19 illustrates the pionic fabric density as a function of distance from the embedded proton pionic cell divided by the pionic fabric density in free space.

In the vicinity of the embedded proton pionic cell, the pionic fabric density is extremely high such that the electron motion via quark exchanges between adjacent pionic cells is inhibited and the electron cannot fall into the coulomb singularity of the proton. On the other limit, far from the embedded proton pionic cell, the electron motion via tunneling between adjacent pionic fabric sites in free space is inhibited since the distances between the pionic fabric cells become too large for the tunneling process. Thus, the density variation of the pionic fabric induced by the hydrogen atom proton confines the electron motion to the atom and prevents the electron fall to the proton coulomb singularity.

10. Pionic QED

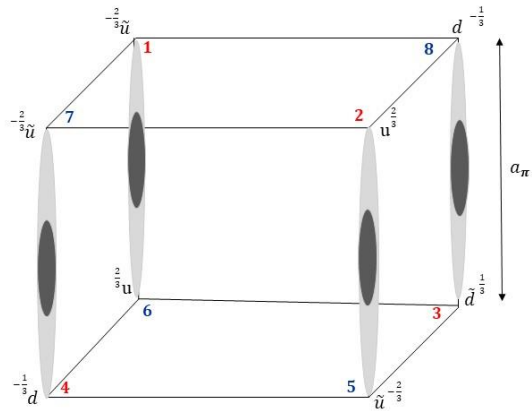
In summary of the pionic fabric and quark molecular dynamics study, we propose a new interpretation of QED based on the pionic fabric structure and dynamics. There are two electron and two positron type structures and dynamics formed by four types of quark exchange dynamics in the pionic fabric. The first embedded electron type I cell structure is shown in figure 20 below formed by introducing a u quark replacing the d quark in vortex 2 for example. The embedded electron cell type I charge is -1.



e^- Type I

Figure 20 illustrates embedded electron type I cell structure.

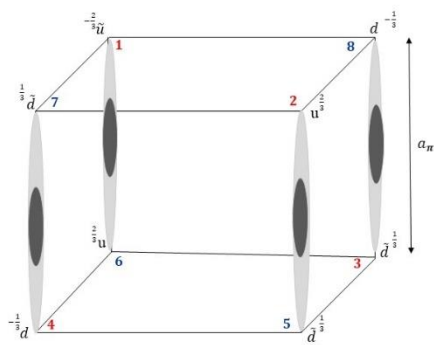
The second embedded electron type II cell structure is shown in figure 21 below formed by introducing a \tilde{d} quark replacing the \tilde{u} quark in vortex 7 for example. The embedded electron cell type II charge is -1.



e^- Type II

Figure 21 illustrates embedded electron type II cell structure.

The first embedded positron type I cell structure is shown in figure 22 below formed by introducing a \tilde{u} quark replacing the \tilde{d} quark in vortex 5 for example. The embedded positron cell type I charge is +1.



e^+ Type I

Figure 22 illustrates embedded positron type I cell structure.

The second embedded positron type II cell structure is shown in figure 23 below formed by introducing a d quark replacing the u quark in vortex 8 for example. The embedded positron cell type II charge is +1.

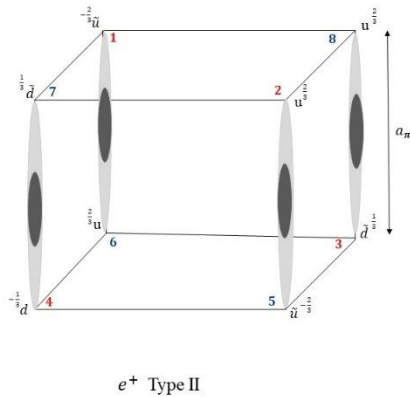


Figure 23 illustrates embedded positron type II cell structure.

QED occurs with the four embedded charged pionic fabric cells by rapid quark exchanges with adjacent pionic fabric cells where charge is transferred from the charged embedded pionic cells to an adjacent neutral pionic fabric cells by quark exchanges via tunneling as described in equations 9 and 10 above. The charge and type of the embedded electrons or positrons are conserved in these quark exchanges. Accordingly, the electron or positron motion occurs by two different mobile particles, a quark exchange dynamic (d and u exchanges) and an antiquark exchange dynamic (\bar{d} and \bar{u} exchanges). The two motions can occur independently in the pion fabric and hence the two electrons with different types can share the same space and an electron cloud forming for example an electron pair in an atom. The length of the embedded electron cell is shorter by a factor of 5 comparing to a neutral pionic fabric cell and we assume that all pionic cells that form the electron cloud are similarly contracted since the quark exchanges are extremely rapid and endlessly repeatable in the cloud.

The energy of the two embedded electron and positron types should be equal to the electron rest mass of 0.511 MeV. However, the energy of type II electron with the same pionic unit cell length is a bit higher 0.554 MeV. By modifying the cell length to $1.669 * 10^{-15}$ meters, comparing to $1.541 * 10^{-15}$ meters of embedded type I electron, we get the expected energy of 0.511 MeV. The small difference in cell lengths means that for two different type electrons that share the electron cloud, in a He atom for example, the embedded pionic fabric cell size would oscillate between the two values dynamically according to the current type of embedded electron or converge to an average value. Since an electron pair with opposite spins in the same atomic orbital is favorable, we assume that the dynamic exchange of both quarks and antiquarks in the pionic fabric cloud stabilizes the shared electron cloud and is favorable compared to a single embedded electron cloud with the d and u exchanges or the \tilde{d} and \tilde{u} exchanges only.

In the case of electron-positron collision and annihilation in the pionic fabric described in equation 17 above, the double quark exchange reaction will annihilate both charges and will generate a neutral pionic fabric cell. The complete electronic cloud that included probably millions of contracted pionic fabric cells will almost instantly expand its volume from the contracted charged pionic fabric cell length of about $1.541 * 10^{-15}$ meters to the value of a pionic fabric cell in the vacuum of about $7.757 * 10^{-15}$ meters. The instant expansion of the pionic fabric by a factor of about 5^3 in volume for millions of pionic fabric cells will generate a significant disturbance in the pionic fabric that may be seen as the expected two 0.511 MeV electromagnetic waves propagating in the vacuum. Note that in the pionic QED interpretation, the electron-positron charge annihilation in the pionic fabric does not annihilate the underlying fundamental building block quarks and antiquarks that are conserved. The quarks and antiquarks are not destroyed nor created, they switch neighbors and remain part of the pionic fabric.

11. Lattice QCD and the Pionic Fabric

Lattice QCD is a non-perturbative computation scheme for the strong force³⁴. Perlovsek et al³⁵ wrote that the only hadron states found so far are two quark mesons and three quark baryons and that no exotic tetraquark, pentaquark, hybrid meson-gluon or molecular meson states have been confirmed beyond doubt yet. However, there are several candidates in the light tetraquarks and hidden charm sectors, and Perlovsek studied with lattice QCD light tetraquarks that may be the experimentally observed σ and κ mesons.

The quark exchange reactions may be seen as hadron scattering reactions. The d and u quarks for example are exchanged between an electron and pion tetraquarks and the scattering reaction is symmetric since the products are the same as the reactants. Equations 9 and 10 above (on page 16) describe tetraquarks scattering reactions where the electron tetraquark is transformed to a pion tetraquark and vice versa. The tetraquark scattering reactions of equations 7, 9, 10 and 17 may be studied with lattice QCD³⁵⁻³⁹ and may allow calculating the mass of the proposed embedded electron pionic cell and the pionic fabric unit cell.

12. Summary

We assume that the answers to the three questions raised above in section 2 are positive and consider them as axioms of the pionic fabric and quark molecular dynamics scheme. Accordingly, both leptons and hadrons are composed particles. The electron is not an elementary point like particle and not a single particle. The pionic fabric cell unit includes 50% quarks and 50% antiquarks and hence the vacuum fabric is not made of ordinary matter particles as Einstein suggested for the gravitational ether⁴⁰. We propose a new interpretation to QED based on the pionic fabric structure and dynamics. Lattice QCD may allow calculating the mass of the proposed embedded electron pionic cell and pionic fabric unit cell.

References

- [1] Helge, K., (2009), “Wave Packets, Compendium of Quantum Physics, Concepts, Experiments, History and Philosophy.”, 828–830, Springer.
- [2] C. G. Darwin, (1927), "Free motion in the wave mechanics", Proceedings of the Royal Society of London. <https://royalsocietypublishing.org/doi/10.1098/rspa.1927.0179>
- [3] P. A. M. Dirac, (1928), “The Quantum Theory of the Electron”, https://www.physics.rutgers.edu/grad/601/QM502_2019/Dirac.pdf
- [4] Kaplan, I. G., (2019). ”Pauli Exclusion Principle and its theoretical foundation”, <https://arxiv.org/pdf/1902.00499>
- [5] Barut, A.O. and Pavsic, M., (1993), “Dirac's shell model of the electron and the general theory of moving relativistic charged membranes”, <https://www.sciencedirect.com/science/article/abs/pii/037026939391136B>
- [6] Feynman, R., “The Feynman Lectures on Physics, Quantum Mechanics”, https://www.feynmanlectures.caltech.edu/III_toc.html
- [7] Feynman, R. and Weinberg, S., (1987), “The Reason for antiparticles” https://www.cambridge.org/core/services/aop-cambridge-core/content/view/9D72E7C9045A9C0797DD952678F03C75/9781107590076c1_p1-60_CBO.pdf/the-reason-for-antiparticles.pdf
- [8] P. A. M. Dirac, (1928), “Lecture on the Foundation of Quantum Mechanics”, <https://mediatheque.lindau-nobel.org/recordings/34222/1965-the-foundations-of-quantum-mechanics>
- [9] Harari, H., (1979), “A Schematic Model of Quarks and Leptons”, https://www.weizmann.ac.il/particle/harari/sites/particle.harari/files/uploads/schematic_model_of_quarks_and_leptons.pdf
- [10] Rom, R., (Apr 2023), “The Quantum Chromodynamics Gas Density Drop and the General Theory of Relativity Ether”, Journal of High Energy Physics, Gravitation and Cosmology, 9, No. 2. <https://www.scirp.org/journal/paperinformation.aspx?paperid=124153>
- [11] Rom, R., (Apr 2023), “Matter Reactors”, Journal of High Energy Physics, Gravitation and Cosmology, 9, No. 2. <https://www.scirp.org/journal/paperinformation.aspx?paperid=124154>
- [12] Rom, R., (Apr, 2024), “Non-Uniform Pion Tetrahedron Aether and Electron Tetrahedron Model”, Journal of High Energy Physics, Gravitation and Cosmology. <https://www.scirp.org/journal/paperinformation?paperid=132602>

- [13] Rom, R., (Jan 2024), “The Pionic Deuterium and the Pion Tetrahedron Vacuum Polarization”, Journal of High Energy Physics, Gravitation and Cosmology, 10, No. 1. <https://www.scirp.org/journal/paperinformation?paperid=130928>
- [14] Rom, R., (May 2024), “QCD’s Low Energy Footprint”, <https://vixra.org/abs/2403.0128>
- [15] Lee, T., (2012), “Vacuum quark condensate, chiral Lagrangian, and Bose-Einstein statistics”, <https://arxiv.org/abs/1206.1637>
- [16] Brodsky, S. B., Shrock, R., (2008), “On Condensates in Strongly Coupled Gauge Theories”, <https://arxiv.org/abs/0803.2541>
- [17] Brodsky, S. B., Roberts, C. D., Shrock, R., Tandy, P.C., (2010), “Essence of the vacuum quark condensate”, <https://arxiv.org/abs/1005.4610>
- [18] Buballa, M., Carignano, S., (2014), “Inhomogeneous chiral condensates”, <https://arxiv.org/abs/1406.1367>
- [19] Byers, N., (1998), “E. Noether’s Discovery of the Deep Connection Between Symmetries and Conservation Laws”, <https://arxiv.org/abs/physics/9807044>
- [20] Burkert, V.D. et al, (2022), “Precision Studies of QCD in the Low Energy Domain of the EIC”, https://www.researchgate.net/publication/365850432_Precision_Studies_of_QCD_in_the_Low_Energy_Domain_of_the_EIC
- [21] Paraoanu, G.S., (2014), ”The Quantum Vacuum”, <https://arxiv.org/abs/1402.1087>
- [22] Peters, A., (2014), “Determination of $\Lambda_{\overline{MS}}$ from the static quark-antiquark potential in momentum space”, Master thesis. https://itp.uni-frankfurt.de/~mwagner/theses/MA_Peters.pdf
- [23] Grabovsky, D, (2021), “The Double Well”, <https://web.physics.ucsb.edu/~davidgrabovsky/files-teaching/Double%20Well%20Solutions.pdf>
- [24] Pengra, D., (2023), “The Inversion Spectrum of Ammonia”, https://courses.washington.edu/phys432/NH3/ammonia_inversion.pdf
- [25] Santos, I. U., (2023), “The zitterbewegung electron puzzle”, https://www.researchgate.net/publication/374257062_The_zitterbewegung_electron_puzzle
- [26] Davis, B.S., (2020), “Zitterbewegung and the Charge of an Electron”, <https://arxiv.org/abs/2006.16003>
- [27] Hui, D., Alqattan, H., Sennary, M., Golubev, N., Hassan, M., (2024), “Attosecond electron microscopy and diffraction”, <https://www.science.org/doi/10.1126/sciadv.adp5805>

- [28] t-Hooft, G., (2004), “Renormalization without Infinities”
<https://arxiv.org/pdf/hep-th/0405032>
- [29] Bergere, M. C., and Zuber, J. Z., (1973), “Renormalization of Feynman Amplitudes and Parametric Integral Representation”
https://www.lpthe.jussieu.fr/~zuber/MesPapiers/bz_CMP74.pdf
- [30] Blechman, A. E., (2002), “Renormalization: Our Greatly Misunderstood Friend”,
<http://www.pha.jhu.edu/~blechman/papers/renormalization/renormalization.pdf>
- [31] Keenan, R.C., Barger, A.J, Cowie, L.L., (2013) “EVIDENCE FOR A ~ 300 MEGAPARSEC SCALE UNDER-DENSITY IN THE LOCAL GALAXY DISTRIBUTION”,
 The Astrophysical Journal, 775:62 (16pp), 2013, September 20.
- [32] Banik, I., (Nov 20, 2023), “Do we live in a giant void? It could solve the puzzle of the Universe’s expansion”, <https://theconversation.com/do-we-live-in-a-giant-void-it-could-solve-the-puzzle-of-the-universes-expansion-216687#:~:text=When%20we%20measure%20the%20expansion,area%20with%20below%20average%20density>).
- [33] Mazurenko, S., Banik, I., Kroupa, P., Haslbauer, M., (Nov 20, 2023), “A simultaneous solution to the Hubble tension and observed bulk flow within $250 h^{-1}$ Mpc”,
<https://arxiv.org/abs/2311.17988>
- [34] Ukawa, A., (2015), “Kenneth Wilson and lattice QCD”,
<https://arxiv.org/abs/1501.04215>
- [35] Boyle, P. et al, (2022), “Lattice QCD and the Computational Frontier”,
<https://arxiv.org/abs/2204.00039>
- [36] Prelovsek, S. et al, (2010), “Lattice study of light scalar tetraquarks with $I = 0, 2, 1/2, 3/2$: are σ and κ tetraquarks?”, <https://arxiv.org/abs/1005.0948>
- [37] Ortiz-Pacheco, E. et al, (2023), “Doubly charmed tetraquark: isospin channels and diquark-antidiquark interpolators”, <https://arxiv.org/abs/2312.13441>
- [38] Alexandrou, C., Berlin, J., Finkenrath, J., Leontiou, T., Wagner, M., (2019), “Tetraquark interpolating fields in a lattice QCD investigation of the $D_{s0}^*(2317)$ meson”,
<https://arxiv.org/abs/1911.08435>
- [39] Meng, L., Chen, Y., Ma, Y., Zhu, S., (2023), “Tetraquark bound states in constituent quark models: benchmark test calculations”, <https://arxiv.org/abs/2310.13354>
- [40] Einstein, A., (1920), “Ether and Relativity”,
https://mathshistory.st-andrews.ac.uk/Extras/Einstein_ether/